DOCTORAL THESIS SUMMARY

CONTRIBUȚII PRIVIND UTILIZAREA PARAMETRILOR $\underline{S}$ ȘI A DIAGRAMEI SMITH ÎN ANALIZA CALITATIVĂ A CIRCUITELOR ANALOGICE

CONTRIBUTIONS REGARDING THE USE OF $\underline{S}$ PARAMETERS AND THE SMITH DIAGRAM IN THE QUALITATIVE ANALYSIS OF ANALOG CIRCUITS

Scientific Coordinator:
Prof. Dr. Eng. Mihai IORDACHE

PhD Student:
Eng. Razvan ASANACHE

2021

TABLE OF CONTENT

1. INTRODUCTION

1.1. Formulating the problem

To characterize linear and nonlinear devices, linearized by portions, in the harmonic mode, the parameters *Z*, *Y*, *H*, *T* etc. are used at low and medium frequencies. When these devices operate at high and very high frequencies these parameters can no longer be used, since they require circuits with certain short-circuited sides or left in the void (interrupted) for taking measurements so that the currents and voltages in the circuit can be calculated.

In order to analyze and simulate analog circuits, in the harmonic regime, at high and very high frequencies, the Scattering parameters are used – usually called *S parameters.* The scattering (distribution) parameters – noted with *S*, are complex numbers, frequency-dependent, associated with a multiport linear system in a harmonic regime. There are conversion formulas between *S* parameters and the classical parameters of the circuit theory (*Z* impedances, *Y* admittances, *H* parameters, fundamental parameters *T* etc.).

In the current doctoral thesis, there were elaborated and implemented advanced procedures for the qualitative analysis, at medium, high and very high frequencies, of the analog circuits, based both on the use of *S* parameters and on the use of the Smith diagram.

The procedures for calculating *S* parameters and the Smith chart use the most advanced calculation programs, such as CADENCE [13, 14, 24], ADS [17, 21, 22, 26], ANSYS și ANSOFT EXTRACTOR Q3D [19, 25, 29], FEKO [20] etc. For a wide class of analog circuits and for different structures of wireless power transfer systems (WPTS) there can be used the specialized programs (dedicated) to the symbolic, numerical – symbolic and numerical simulation of the linear and / or nonlinear analog circuits, elaborated within the Department of Electrotechnics –University Politehnica of Bucharest, ACAP – Analogue Circuit Analysis Program, SCAP – Symbolic Circuit Analysis Program, SYTFG – SYmbolic Transfer Function Generation and SYSEG – SYmbolic State Equation Generation, [10, 15, 16], which allow the simulation, in any operating mode, of complex analog circuits.

The generation of *S* parameters for linear analogue circuits and for nonlinear analog circuits, linearized on portions around a point of operation, under precise polarization and temperature conditions of electronic devices, can be carried out by means of small signal simulations.

For the generation of *S* parameters for nonlinear circuits, the LSSP – Large-Signal S-Parameter Simulation simulator is used, which uses the method of analyzing the *harmonic balance.* Simulation based on the harmonic balance method is a *large signal* simulation, to which solutions also include the effects of nonlinearities of electronic components.

S parameters, both small and large signals, are defined as ratios between incident and reflected waves.

This doctoral thesis aims to develop efficient algorithms and high-performance programs of qualitative analysis, based on the efficient use of *S* parameters and Smith diagram, for multiport analog circuits and magnetically coupled coil systems that are used in wireless power transfer systems. Electromagnetic devices operating in dynamic regimes from the perspective of their treatment, allow the use of analysis techniques specific to electrical circuits.

The main objectives of this doctoral thesis are:

✓ Correct definition of S parameters and elaboration of efficient procedures for their automatic calculation.

✓ Use of S parameters in the analysis of two-port and/or multiport circuits and magnetically coupled coil systems, used in wireless power transfer systems, and considered as two-port circuits.

✓ The use of S parameters in the analysis of the stability of wireless active power transmission systems and in the study of the stability of electrical circuits widely used in practice.

✓ Correct definition of the figure of merit kQ and its use in the analysis of the efficiency of power transfer in the two-port electrical systems.

1.2. Structure and content of the thesis

The paper "**Contributions regarding the use of *S* parameters and the Smith Diagram in the qualitative analysis of analog circuits**" is structured on the following chapters:

Chapter 1 – Introduction, where were exposed the current state of the use of S parameters and the Smith diagram in the analysis, synthesis and design of analog circuits, the purpose and objective of this work, the structure of the paper and the results' dissemination through the published scientific articles.

Chapter 2 – Definition of S parameters and their automatic calculation procedures, where is presented the definition *of S* parameters, using the theory of electrical circuits, and also are exposed some efficient procedures for calculating these parameters.

Chapter 3 – The use of S parameters in the analysis of two-port circuits, where the essential parameters of any two-port circuit are determined according to S parameters and there is presented the practical way of using these parameters in the efficiency of the information transmission and propagation processes and in the efficiency of the active power transfer from the input of the passive linear quadrupoles to the loads connected to their output.

Chapter 4 – The use of S parameters in the stability of wireless electromagnetic energy transfer systems, which presents the stability analysis of wireless electromagnetic energy transfer systems in terms of analysis of specific parameters that influence stability, calculated according to S parameters.

Chapter 5 – Calculation of the kQ figure of merit and the properties of wireless electromagnetic power transfer systems, which presents how to calculate the factor of merit and its role in the wireless transfer of the electromagnetic power.

Chapter 6 – Conclusions, which presents the general conclusions resulting from the research carried out on the use of the S parameters and the Smith diagram in the qualitative analysis of analog circuits, the original contributions of the author of the work and the perspectives of further development of the chosen research topic.

1.3. Dissemination of results

The dissemination of the results was achieved by publishing a number of 8 articles within specialized conferences and in the Scientific Bulletin of the University Politehnica of Bucharest, as follows:

• *Mihai Iordache, Marilena Stănculescu, Dragoş Niculae, Maria-Lavinia Iordache (Bobaru),* ***Răzvan Asanache***, "Switched Networks Analysis with Inconsistent Initial Conditions", Modern Power Systems, Cluj, 06-09.06.2017, PID4766833, coauthor.

• *Ciprian Curteanu, Maria-Lavinia Iordache (Bobaru),* ***Răzvan Asanache****, Mihai Iordache, Marilena Stanculescu*, "*S*-Parameters' utilization in electrical

quadrupoles analysis", Electronics, Computers and Artificial Intelligence, Targoviste, 29.06-01.07.2017, paper 61, <u>coauthor</u>.

- ***Răzvan Asanache**, Mihai Iordache, Dragoş Niculae, Marilena Stănculescu, Maria Lavinia Bobaru, Victor Bucată*, "The computation of the *kQ*-product and properties of wireless power transfer systems", International Conference on Applied and Theoretical Electricity, Craiova, 04-06.10.2018, ID134, <u>lead author</u>.

- ***Răzvan Asanache**, Mihai Iordache, Dragoş Niculae, Marilena Stănculescu, Lavinia Bobaru, Victor Bucată*, "On Circuit Analysis and Simulation of Networks with Nullors", Modern Power Systems, Cluj, 21-23.05.2019, ID169, <u>lead author</u>.

- ***Răzvan Asanache**, Cristina Mihaela Turcu, Mihai Iordache*, "Automatic Generation of Linear Quadrupole Parameters", U.P.B. Scientific Bulletin Series C: Electrical Engineering and Computer Science, iunie 2020, ID: 9381, <u>lead author</u>.

- ***Răzvan Asanache**, Mihai Iordache, Mihaela Cristina Turcu, Alexandru Grib, Lucian Vasile Ene, Diana Ramona Sănătescu*, "Wireless Charging Systems for Electrical Vehicle Batteries", Electronics, Computers and Artificial Intelligence, 2020, e-Session, ID: 55, <u>lead author</u>.

- *Mihaela Cristina Turcu, Mihai Iordache, **Răzvan Asanache**, Alexandru Grib, Teodor Cătălin Bibirică*, "Smart Integrative System for the Battery Balance Monitoring", Electronics, Computers and Artificial Intelligence, 2020, e-Session, ID: 56, <u>coauthor</u>.

- *Alexandru Grib, Mihai Iordache, **Răzvan Asanache**, Mihaela Cristina Turcu, Teodor Cătălin Bibirică*, "Smart Battery Monitoring System Software Design", Electronics, Computers and Artificial Intelligence, 2020, e-Session, ID: 97, <u>coauthor</u>.

1.4. List of abbreviations

- e.m.f. – electromotive force
- ESR – Equivalent Scalar Resistance
- FoM – Figure of Merit
- LSSP Simulation – Large-Signal *S*-Parameter Simulation
- MEMS – Micro-Electro-Mechanical System
- MNM – Modified Nodal Method
- PPMCR – Parallel-Parallel Magnetic Coupled Resonator
- PSMCR – Parallel-Series Magnetic Coupled Resonator
- SCAP – Symbolic Circuit Analysis Program
- SPMCR – Series-Parallel Magnetic Coupled Resonator
- SSMCR – Series-Series Magnetic Coupled Resonator
- SWR – Standing Wave Ratio
- SYSEG – SYmbolic State Equation Generation
- SYTFG – SYmbolic Transfer Function Generation
- VCO – Voltage Controlled Oscillator
- VNA – Vector Network Analyzer
- WPTS – Wireless Power Transfer Systems

2. DEFINITION OF $\underline{S}$ PARAMETERS AND THEIR AUTOMATIC CALCULATION PROCEDURES

2.1. Introduction

To characterize linear and nonlinear devices, linearized by portions, in the harmonic mode, the parameters $\underline{Z}$, $\underline{Y}$, $\underline{H}$, $\underline{T}$ etc. are used at low and medium frequencies. When these devices operate at high and very high frequencies these parameters can no longer be used, since they require circuits with certain short-circuited sides or left in the void (interrupted) for taking measurements so that the currents and voltages in the circuit can be calculated.

In order to analyze and simulate analog circuits, in the harmonic regime, at high and very high frequencies, the Scattering parameters are used – usually called $\underline{S}$ *parameters.* The scattering (distribution) parameters – noted with $\underline{S}$, are complex numbers, frequency-dependent, associated with a multiport linear system in a harmonic regime.

There are conversion formulas between $\underline{S}$ parameters and the classical parameters of the circuit theory ($\underline{Z}$ impedances, $\underline{Y}$ admittances, $\underline{H}$ parameters, fundamental parameters $\underline{T}$ etc.).

This chapter presents the correct definition of $\underline{S}$ parameters, using the theory of electrical circuits, and also exposes some procedures for calculating these parameters. The procedures for calculating the $\underline{S}$ parameters use the most advanced calculation programs, such as CADENCE [13, 14, 24], ADS [17, 21, 22, 26], ANSYS și ANSOFT EXTRACTOR Q3D [19, 25, 29], FEKO [20] etc.

2.2. $\underline{S}$ parameters definition

In order to correctly define the $\underline{S}$ parameters for a two-port structure, consider the circuit in figure 2.1.
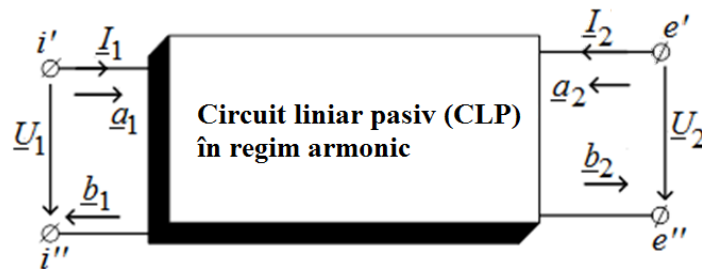
Fig. 2.1. Circuit used to define $\underline{S}$ parameters.

Starting from the change of the pairs of variables ($\underline{U}_1$, $\underline{I}_1$) and ($\underline{U}_2$, $\underline{I}_2$) with the pairs ($\underline{a}_1$, $\underline{b}_1$) and respectively ($\underline{a}_2$, $\underline{b}_2$), according to the relations:

$$\underline{U}_1 = \sqrt{Z_0}\left(\underline{a}_1 + \underline{b}_1\right), \quad \underline{I}_1 = \frac{1}{\sqrt{Z_0}}\left(\underline{a}_1 - \underline{b}_1\right)$$

$$\underline{U}_2 = \sqrt{Z_0}\left(\underline{a}_2 + \underline{b}_2\right), \quad \underline{I}_2 = \frac{1}{\sqrt{Z_0}}\left(\underline{a}_2 - \underline{b}_2\right),$$

(2.1)

where Z_0 is a positive real variable, called – *reference (characteristic) impedance* and considering that the $\underline{S}$ parameters of a two-port structure (fig. 2.1) satisfy the following equations between incident and reflected signals:

$$\underline{b}_1 = \underline{S}_{11}\underline{a}_1 + \underline{S}_{12}\underline{a}_2$$
$$\underline{b}_2 = \underline{S}_{21}\underline{a}_1 + \underline{S}_{22}\underline{a}_2$$

(2.2)

the four $\underline{S}$ parameters associated with a linear two-port circuit can be defined as follows:

- $\underline{S}_{11}$ **parameter**

$$\underline{S}_{11} = \frac{\underline{b}_1}{\underline{a}_1}\Bigg|_{\substack{\underline{a}_2=0 \Leftrightarrow \underline{U}_2=-Z_c\underline{I}_2 \\ \underline{Z}_s=Z_c, \underline{U}_1=\underline{E}_i-Z_c\underline{I}_1}} = \frac{\underline{U}_1 - Z_c\underline{I}_1}{\underline{U}_1 + Z_c\underline{I}_1}\Bigg|_{\substack{\underline{a}_2=0 \Leftrightarrow \underline{U}_2=-Z_c\underline{I}_2 \\ \underline{Z}_s=Z_c, \underline{U}_1=\underline{E}_i-Z_c\underline{I}_1}} = \frac{\underline{E}_i - 2Z_c\underline{I}_c}{\underline{E}_i} = 1 - 2\underline{A}_{1i},$$

(2.3)

where $\underline{A}_{1i} = \dfrac{Z_c\underline{I}_1}{\underline{E}_i}\Bigg|_{\underline{U}_2=-Z_c\underline{I}_2, \underline{Z}_s=Z_c}$ is the transfer (amplification) factor in voltage, calculated when

at the input port of the circuit is connected the e.m.f. $\underline{E}_i$ in series with the input impedance $\underline{Z}_i = Z_c$, and at output port is connected the impedance $\underline{Z}_e = \underline{Z}_s = Z_c$.

- $\underline{S}_{12}$ **parameter**

$$\underline{S}_{12} = \frac{\underline{b}_1}{\underline{a}_2}\Bigg|_{\substack{\underline{a}_1=0 \Leftrightarrow \underline{U}_1=-Z_c\underline{I}_1 \\ \underline{Z}_i=Z_c, \underline{Z}_s=Z_c}} = \frac{\underline{U}_1 - Z_c\underline{I}_1}{\underline{U}_2 + Z_c\underline{I}_2}\Bigg|_{\substack{\underline{a}_1=0 \Leftrightarrow \underline{U}_1=-Z_c\underline{I}_1 \\ \underline{Z}_i=Z_c, \underline{Z}_s=Z_c}} = \frac{-2Z_c\underline{I}_1}{\underline{E}_e} = -2\underline{A}_{ie},$$

(2.4)

unde $\underline{A}_{ie} = \dfrac{Z_c\underline{I}_1}{\underline{E}_e}\Bigg|_{\underline{U}_1=-Z_c\underline{I}_1, \underline{Z}_s=Z_c}$ is the transfer (amplification) factor in voltage, when the

characteristic impedance Z_c is connected at the input port ($\underline{E}_i$ being zero) and at the output port is connected the impedance $\underline{Z}_s = Z_c$ in series with e.m.f. $\underline{E}_e$.

- $\underline{S}_{21}$ **parameter**

$$\underline{S}_{21} = \frac{\underline{b}_2}{\underline{a}_1}\Bigg|_{\substack{\underline{a}_2=0 \Leftrightarrow \underline{U}_2=-Z_c\underline{I}_2 \\ \underline{Z}_i=Z_c, \underline{Z}_s=Z_c, \underline{U}_1=\underline{E}_i-Z_c\underline{I}_1}} = \frac{\underline{U}_2 - Z_c\underline{I}_2}{\underline{U}_1 + Z_c\underline{I}_1}\Bigg|_{\substack{\underline{a}_2=0 \Leftrightarrow \underline{U}_2=-Z_c\underline{I}_2 \\ \underline{Z}_i=Z_c, \underline{Z}_s=Z_c, \underline{U}_1=\underline{E}_i-Z_c\underline{I}_1}} = \frac{-2Z_c\underline{I}_2}{\underline{E}_i} = -2\underline{A}_{ei},$$

(2.5)

unde $\underline{A}_{ei} = \dfrac{Z_c\underline{I}_2}{\underline{E}_i}\Bigg|_{\underline{U}_2=-Z_c\underline{I}_2, \underline{Z}_i=Z_c, \underline{Z}_s=Z_c}$ is the transfer (amplification) factor in voltage from the

output port to the input one, according to the conditions mentioned in the expression (2.5).

- $\underline{S}_{22}$ **parameter**

$$\underline{S}_{22} = \frac{\underline{b}_2}{\underline{a}_2}\Bigg|_{\substack{\underline{a}_1=0 \Leftrightarrow \underline{U}_1=-Z_c\underline{I}_1 \\ \underline{Z}_i=Z_c, \underline{Z}_s=Z_c, \underline{U}_2=\underline{E}_e-Z_c\underline{I}_2}} = \frac{\underline{U}_2 - Z_c\underline{I}_2}{\underline{U}_2 + Z_c\underline{I}_2}\Bigg|_{\substack{\underline{a}_1=0 \Leftrightarrow \underline{U}_1=-Z_c\underline{I}_1 \\ \underline{Z}_i=Z_c, \underline{Z}_s=Z_c, \underline{U}_2=\underline{E}_e-Z_c\underline{I}_2}} =$$
$$= \frac{\underline{E}_e - 2Z_c\underline{I}_2}{\underline{E}_e} = 1 - 2\underline{A}_{2e}$$

(2.6)

unde $\underline{A}_{2e} = \dfrac{Z_c\underline{I}_2}{\underline{E}_e}\Bigg|_{\underline{U}_1=-Z_c\underline{I}_1, \underline{Z}_s=Z_c}$ is the transfer (amplification) factor in voltage when at the input

port is connected the characteristic impedance Z_c ($\underline{E}_i$ being zero) and at the output port is connected the impedance $\underline{Z}_s = Z_c$ in series with the e.m.f. $\underline{E}_e$.

The reflection factor $\underline{S}_{11}$ and the transmission factor $\underline{S}_{21}$ can be measured with the vector network analyzer (VNA) [10, 13 – 16].

The generation of $\underline{S}$ parameters for linear analogue circuits and for nonlinear analog circuits, linearized on portions around a point of operation, under precise polarization and

temperature conditions of electronic devices, can be carried out by means of small signal simulations, [17, 29].

A linear circuit can be analyzed as a multiport network. Each port is sequentially excited by small signals and the response is measured and transformed into $\underline{S}$ parameters.

The $\underline{S}$ parameters for the two-port circuit shown in Figure 2.1 have the following meanings:

- $\underline{S}_{11}$ – is the reflection coefficient at the port 1.
- $\underline{S}_{22}$ – is the reflection coefficient at the port 2.
- $\underline{S}_{21}$ – is the transmission coefficient from the port 1 to the port 2.
- $\underline{S}_{12}$ – is the transmission coefficient from the port 2 to the port 1.

$\underline{S}$ parameters are defined in relation to a characteristic impedance that is generally 50 Ω.

For the generation of $\underline{S}$ parameters for nonlinear circuits, the LSSP – Large-Signal S-Parameter Simulation simulator is used [16, 18], which uses the method of analyzing the *harmonic balance.* Simulation based on the harmonic balance method is a *large signal* simulation, to which solutions also include the effects of nonlinearities of electronic components. $\underline{S}$ parameters, both small and large signals, are defined as ratios between incident and reflected waves, [10, 14].

2.3. $\underline{S}$ parameters' calculation procedure

For the calculation of the $\underline{S}$ parameters, for different structures of wireless power transfer systems, either the modified nodal equations, generated by the *SCAP* program, or the state equations, generated by the SYSEG program, can be used, [10, 15, 16].

In the following, the algorithm for calculating the $\underline{S}$ parameters for the configuration of the resonator with series-series connection will be presented, when, for the generation of the modified nodal equations, the SCAP program is used (the results are identical to those obtained with the SYSEG program), [10, 15, 16

The validation of the results obtained with the SCAP and SYSEG programs was made by comparing them with those calculated with the ADS program [17, 21].

The system consisting of the two magnetically coupled resonators used in the wireless transfer of electromagnetic power can be considered as a passive linear two-port circuit represented in figure 2.1.

The active power received at the input port has the expression:

$$P_1 = P_{in} = \mathrm{Re}\left(\underline{U}_1 \cdot \underline{I}_1^*\right) = \left|\underline{a}_1\right|^2 - \left|\underline{b}_1\right|^2. \tag{2.7}$$

The active power supplied to the output port has the expression:

$$P_2 = P_L = -\mathrm{Re}\left(\underline{U}_2 \cdot \underline{I}_2^*\right) = -\left|\underline{a}_2\right|^2 + \left|\underline{b}_2\right|^2. \tag{2.8}$$

Power losses are given by the difference between the power P_1 and the power of P_2:

$$P_{loss} = P_1 - P_2 = \left|\underline{a}_1\right|^2 + \left|\underline{a}_2\right|^2 - \left|\underline{b}_1\right|^2 - \left|\underline{b}_2\right|^2 = \left(\mathbf{a}^*\right)^{\mathrm{t}} \cdot \underline{\mathbf{a}} - \left(\mathbf{b}^*\right)^{\mathrm{t}} \cdot \underline{\mathbf{b}}, \tag{2.9}$$

where $\underline{\mathbf{a}} = \begin{bmatrix} \underline{a}_1 \\ \underline{a}_2 \end{bmatrix}$ and $\underline{\mathbf{b}} = \begin{bmatrix} \underline{b}_1 \\ \underline{b}_2 \end{bmatrix}$ and considering $\underline{b} = \underline{S} * \underline{a}$, where $\underline{S} = \begin{bmatrix} \underline{S}_{11} & \underline{S}_{12} \\ \underline{S}_{21} & \underline{S}_{22} \end{bmatrix}$.

Active power transmission efficiency from the transmitting coil to the load can be calculated with the relation:

$$\eta_{21} = \frac{P_2}{P_1} \cdot 100. \tag{2.10}$$

The efficiency of transmitting signals from the transmitting coil to the load has the expression:

$$\eta_{21\_S_{21}} = \underline{S}_{21} \cdot \underline{S}_{21}^* \cdot 100 = \left| \underline{S}_{21} \right|^2 \cdot 100 , \tag{2.11}$$

and the efficiency of signal transmission from the receiving coil to the generator is calculated with the relation:

$$\eta_{12\_S_{12}} = \underline{S}_{12} \cdot \underline{S}_{12}^* \cdot 100 = \left| \underline{S}_{12} \right|^2 \cdot 100 . \tag{2.12}$$

2.4. Algorithm for calculating $\underline{S}$ parameters for the series-series configuration

Below are presented the important steps of the algorithm for generating $\underline{S}$ parameters ($\underline{S}_{11}$, $\underline{S}_{12}$, $\underline{S}_{21}$ and $\underline{S}_{22}$) for the magnetically coupled resonator with series-series connection, shown in Figure 2.2.
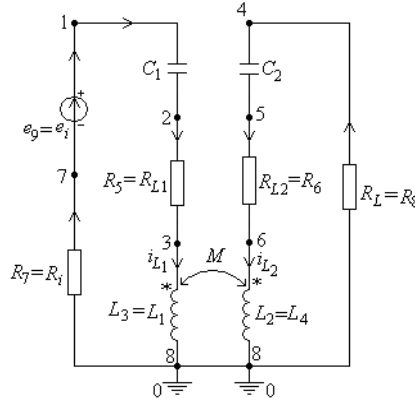

Fig. 2.2. The circuit used to generate the parameters $\underline{S}_{11\_ss}$ and $\underline{S}_{21\_ss}$.

P1. The calculation of parameters $\underline{S}_{11\_ss}$ and $\underline{S}_{21\_ss}$

For the calculation of parameters $\underline{S}_{11} = 1.0 - 2.0*Zc*\underline{I}1/\underline{E}_i$ and $\underline{S}_{21} = -2.0*\underline{A}ei$ there is analyzed in the harmonic regime, with the SCAP program, the circuit from figure 2.2, with the condition $Ri = R_L = Zc$ (Rc).

P2. The calculation of the efficiency eta$_{21\_f\_ss}$ expression for the following numerical values of the parameters: C1=0.188e-06 F; C2=0.4e-06 F; L1=50.0e-06 H; L2=24.0e-06 H; M=8.4896e-06 H; RL1=0.0162 Ω; RL2=0.011 Ω; Ri=1.5 Ω; RL=6.0 Ω; ei=100.0 V; kn=0.25.

P3. The factor $\underline{S}_{11\_ss}$, considering $R_c = 6$ ohms

P4. The parameter $\underline{S}_{21\_ss}$ is the most important $\underline{S}$ coefficient because $\underline{S}_{21}{}^2$ represents the efficiency of signal transmission for resonators SSMCR, from input to output.
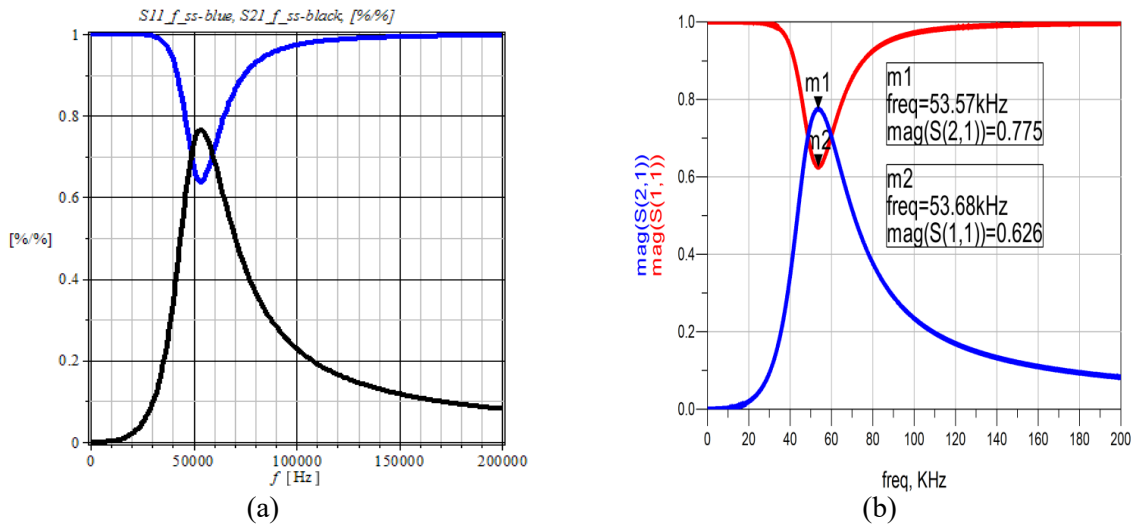

(a)

(b)

Fig. 2.3. Variations with the frequency of parameter modules $\underline{S}_{11\_f\_ss}$ and $\underline{S}_{21\_f\_ss}$:
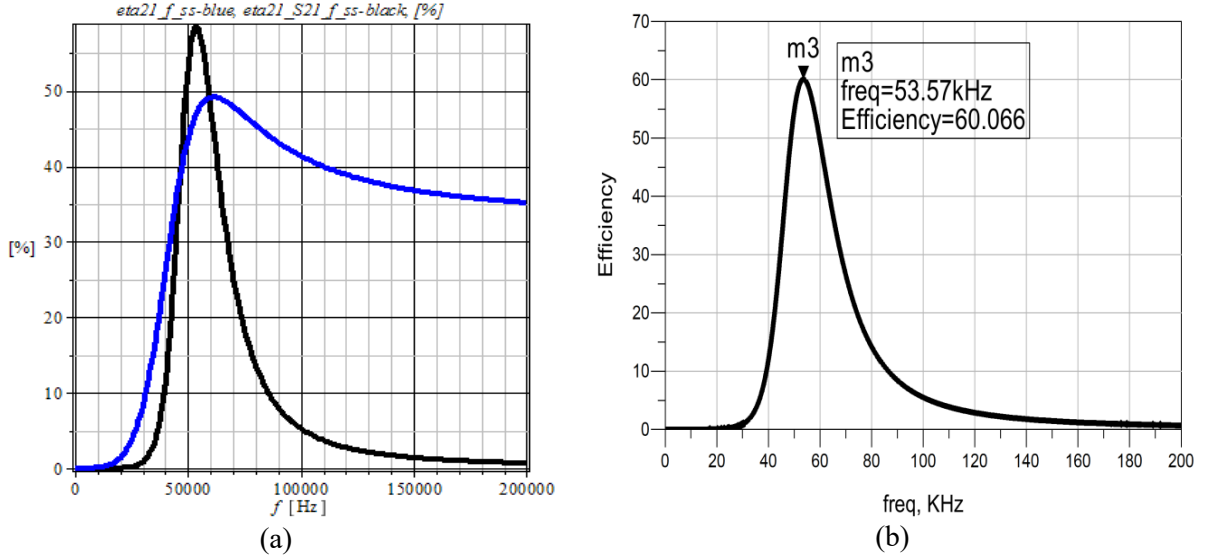a) Calculated with programs SCAP and SYSEG; b) Calculated with ADS program.

(a)   (b)

Fig. 2.4. Variations with the frequency of efficiencies $eta_{21\_f\_ss}$ and $eta_{21\_S21\_f\_ss}$:
a) Calculated with programs SCAP and SYSEG; b) $eta_{21\_S21\_f\_ss}$ calculated with ADS program.

P5. The calculation of parameters $\underline{S}_{12}=-2.0*\underline{A}_{ie}$ and $\underline{S}_{22}=1.0-2.0*\underline{A}_{ie}$.

To determine these distribution factors, the resonator output port is connected to a generator is fed to the exit gate and to the input port there is connected Rc (generally Z_{1_c}).
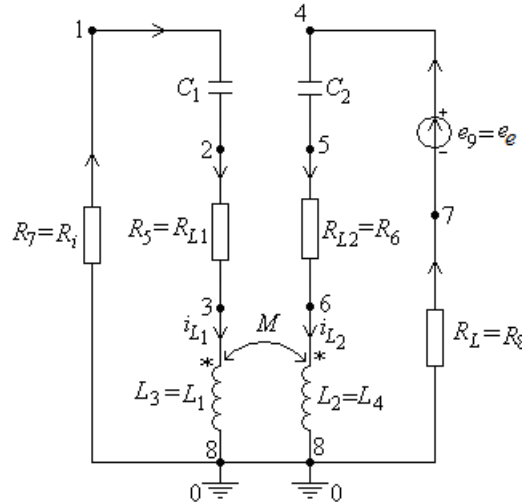

Fig. 2.5. The circuit used to generate the parameters $\underline{S}_{12\_ss}$ and $\underline{S}_{22\_ss}$.

P6. The calculation of the efficiency $eta_{12\_f\_ss}$ expression for the following numerical values of the parameters: C1=0.188e-06 F; C2=0.4e-06 F; L1=50.0e-06 H; L2=24.0e-06 H; M=8.4896e-06 H; RL1=0.0162 Ω; RL2=0.011 Ω; Ri=1.5 Ω; RL=6.0 Ω; eo=100.0 V; kn=0.25.

P7. The factor $\underline{S}_{22\_ss}$, considering $Rc = 6$ ohms

P8. The parameter $\underline{S}_{12\_ss}$ is the most important $\underline{S}$ coefficient because $\underline{S}_{12}{}^2$ represents the efficiency of signal transmission for resonators SSMCR, from the output to the input.
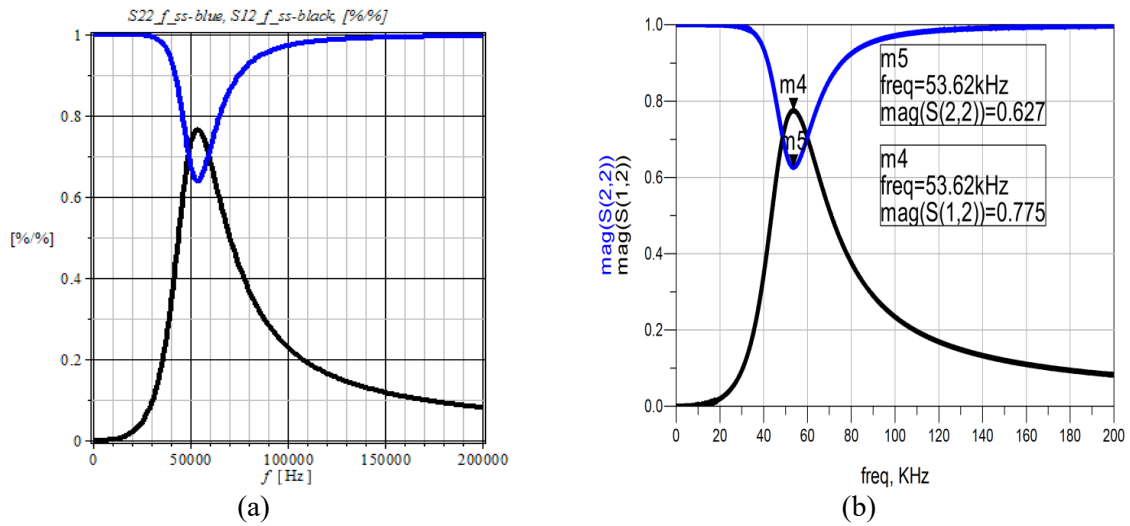
11

(a)

(b)

Fig. 2.6. Variations with the frequency of parameter modules $S_{22\_f\_ss}$ and $S_{12\_f\_ss}$:
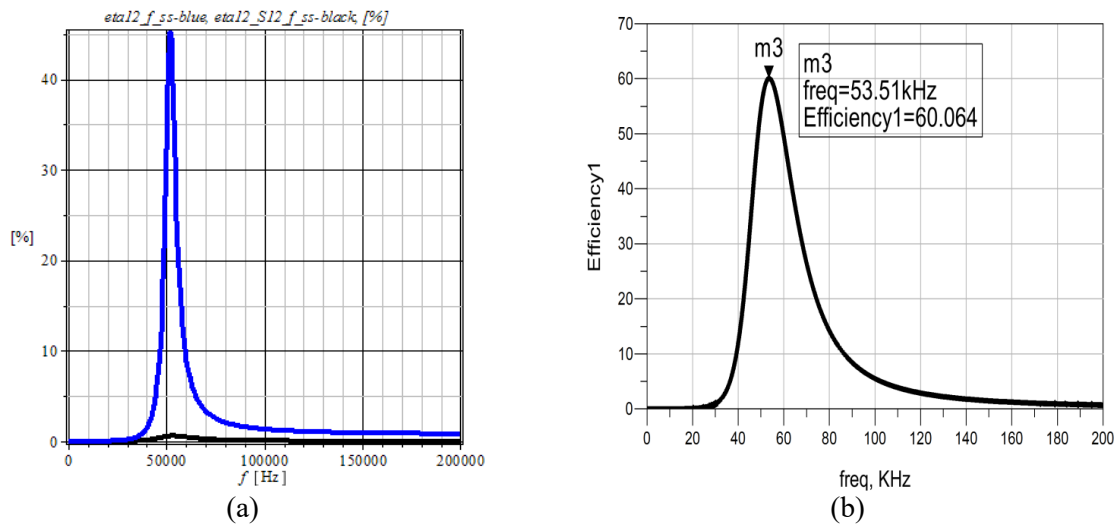a) Calculated with programs SCAP and SYSEG; b) Calculated with ADS program.

(a)

(b)

Fig. 2.7. Variations with the frequency of efficiencies $eta_{12\_f\_ss}$ and $eta_{12\_S12\_f\_ss}$:
a) Calculated with programs SCAP and SYSEG; b) $eta_{12\_S12\_f\_ss}$ calculated with ADS program.

In order to validate the results obtained with the SCAP program, there are considered two magnetically coupled resonators with series-series connection represented in figure 2.10, where the two coils L_3 and L_4 are two identical coaxial coils, as shown in Figure 2.11.
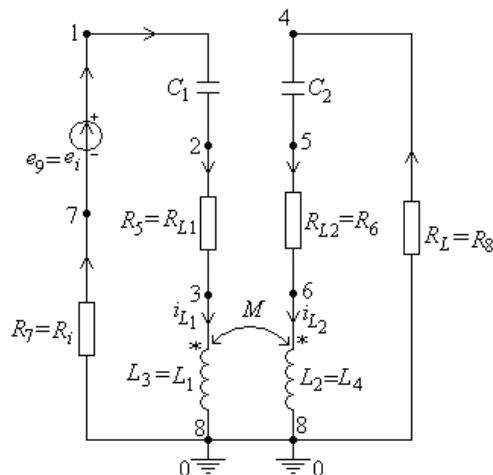

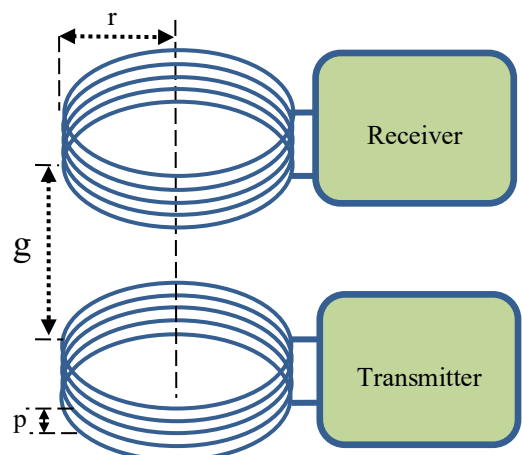**Fig. 2.10.** Two magnetically coupled resonators with series-series connection.

Fig. 2.11. Geometry of coils [15, 16].

12

Using the SYSEG program [10, 15, 16], the circuit state equations from figure 2.10 in fully symbolic form are obtained.

The most important $\underline{S}$ parameters are the reflection factor $\underline{S}_{11}$ and the transmission factor $\underline{S}_{21}$ because the efficiency of reflected signals is $\eta_{11} = S_{11}^{2} \times 100\,(\%)$, and the efficiency for the transmission signals has the expression $\eta_{21\_S_{21}} = S_{21}^{2} \times 100$, [10, 13 – 16].

Active power transmission efficiency $\eta_{21\_f\_ss}$ from transmitter to receiver is as follows:

$$\eta_{21\_f\_ss} = \frac{P_{R8\_f\_ss}}{P_{Rit\_f\_ss} + P_{Rlt\_f\_ss}} \times 100, \qquad (2.13)$$

where: $P_{R8\_f\_ss}$, $P_{Rit\_f\_ss}$, and $P_{Rlt\_f\_ss}$ are the powers dissipated in the resistors R_8, $(R_5 + R_7)$ and respectively $(R_6 + R_8)$. Figure 2.12 shows the variations with the frequency of the efficiencies $\eta_{21\_f\_ss}$ – blue, $\eta_{21\_S21\_f\_ss\_Q3D}$ - blackL and $\eta_{21\_S21\_f\_ss\_Q3D}$ – blackP depending on the distance *g* between the transmitter coil and the receiver coil.

Figure 2.12 shows the variations with the frequency of the efficiencies eta$_{21\_f\_ss}$, eta$21_{\_S21\_f\_ss\_p}$ and eta$21_{\_S21\_f\_ss\_Q3D}$, for each distance *g,* two values for mutual inductiveness are considered, one analytically determined [16], Mp, and the other one obtained with the program ANSOFT EXTRACTOR Q3D – noted M_{Q3D}.
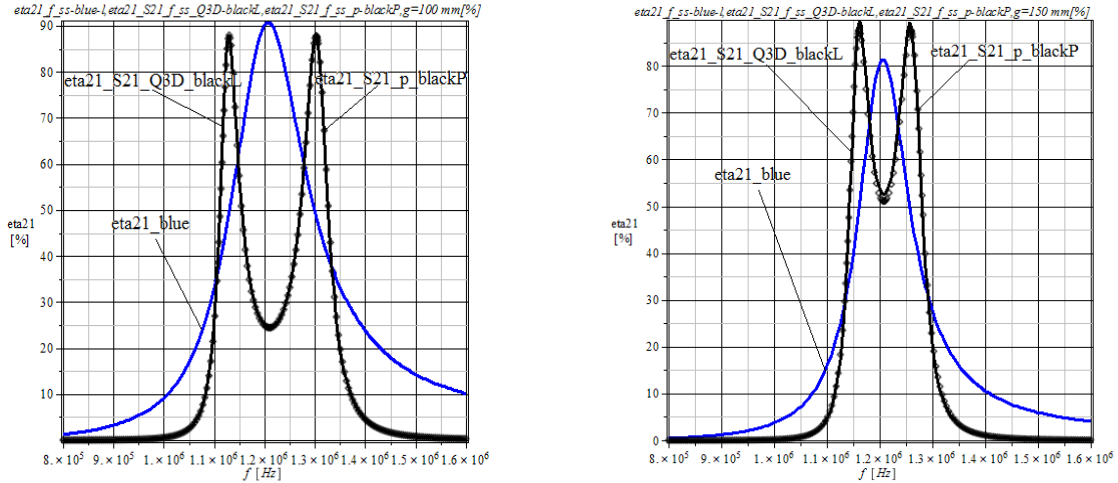
a) $g = 100$ mm, $M_p = 2.5$ µH, $k_p = 0.14933$, $M_{Q3D} = 2.468$ µH, $k_{Q3D} = 0.14742$.

b) $g = 150$ mm, $M_p = 1.5$ µH, $k_p = 0.094376$, $M_{Q3D} = 1.4898$ µH, $k_{Q3D} = 0.088988$.
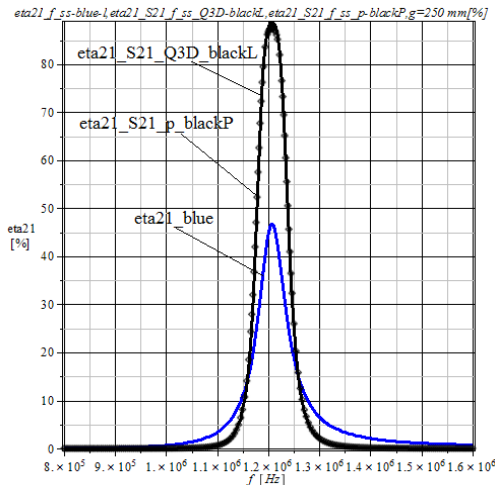
c) $g = 250$ mm, $M_p = 0.65$ µH, $k_p = 0.038825$, $M_{Q3D} = 0.64191$ µH, $k_{Q3D} = 0.03834$.
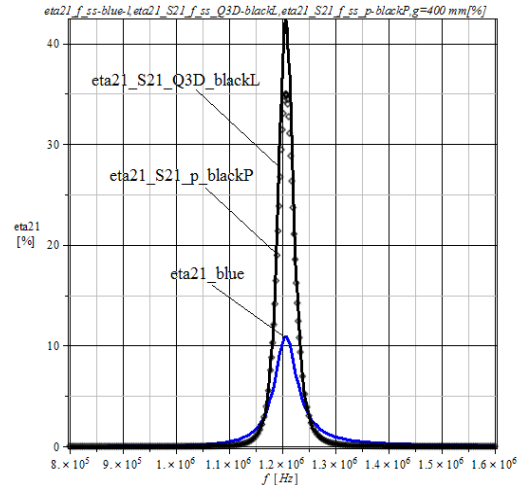
d) $g = 400$ mm, $M_p = 0.24$ µH, $k_p = 0.014335$, $M_{Q3D} = 0.23558$ µH, $k_{Q3D} = 0.01407$

Fig. 2.12. Variations with the frequency of efficiencies $\eta_{21\_f\_ss}$ – blue, $\eta_{21\_S21\_f\_ss\_Q3D}$ - blackL and $\eta_{21\_S21\_f\_ss\_p}$ - blackP.

To validate the results obtained with the SYSEG and SCAP programs, for the resonator shown in figure 2.10, there will be calculated the parameters $\underline{S}_{11\_f\_ss}$, $\underline{S}_{21\_f\_ss}$ and $\eta_{21\_S21\_f\_ss} = 100 \cdot \underline{S}_{21\_f\_ss} \cdot \underline{S}^*_{21\_f\_ss}$ depending on the distance g between the coils, both with these programs and with the ADS program. For each distance g is considered the mutual inductiveness M, obtained with the program Ansoft ExtractorQ3D – noted M_{Q3D}. Figures 2.13 – 2.15 present variations with the frequency of sizes abs($\underline{S}_{11\_f\_ss}$), abs($\underline{S}_{21\_f\_ss}$), abs($\underline{S}_{22\_f\_ss}$), abs($\underline{S}_{12\_f\_ss}$) and $\eta_{21\_f\_ss}$, $\eta_{21\_S21\_f\_ss}$, $\eta_{12\_S12\_f\_ss}$. Because the results obtained with the SYSEG and SCAP programs are identical, figures 2.13 – 2.15 will present the results achieved with one of the two programs.

Calculated with programs SCAP and SYSEG | Calculated with ADS program

(a) (b)
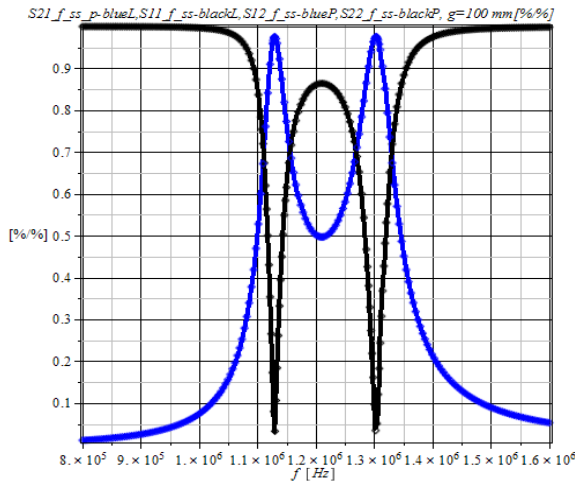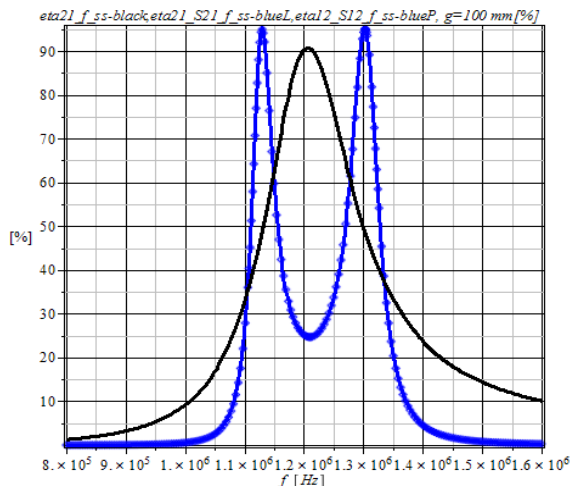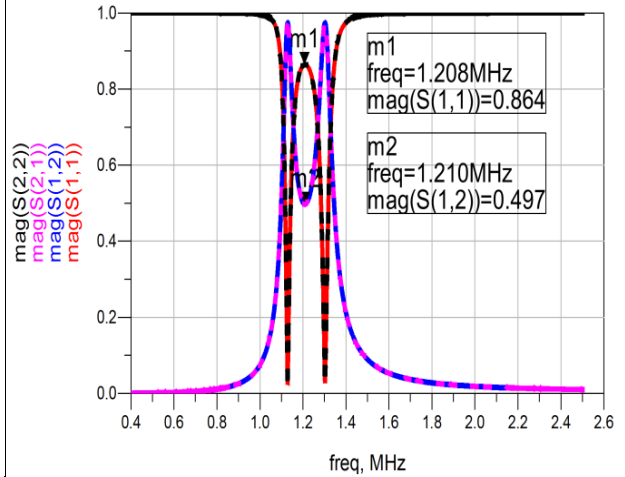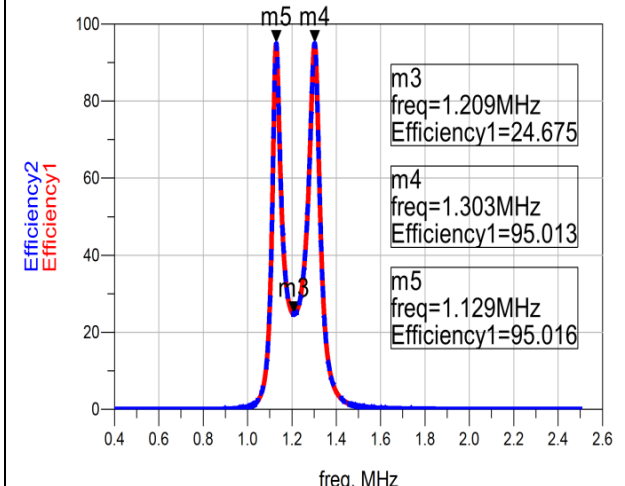
(c) (d)

Fig. 2.13. Variations with the frequency of parameter modules $\underline{S}_{11\_f\_ss}$, $\underline{S}_{21\_f\_ss}$, $\underline{S}_{22\_f\_ss}$ and $\underline{S}_{12\_f\_ss}$: a)Calculated with programs SCAP and SYSEG; b)Calculated with ADS program and variations in the frequency of efficiencies $eta_{21\_f\_ss}$, $eta_{21\_S21\_f\_ss}$ and $eta_{12\_S12\_f\_ss}$; c)Calculated with programs SCAP and SYSEG; d)$eta_{21\_S21\_f\_ss}$ and $eta_{12\_S12\_f\_ss}$ calculated with ADS, $g = 100$ mm, $M_{Q3D} = 2.468$ μH, $k_{Q3D} = 0.14742$.

(a)

(b)

(c)

(d)

Fig. 2.14. Variations with the frequency of parameter modules $\underline{S}_{11\_f\_ss}$, $\underline{S}_{21\_f\_ss}$, $\underline{S}_{22\_f\_ss}$ and $\underline{S}_{12\_f\_ss}$:
a)Calculated with programs SCAP and SYSEG; b)Calculated with ADS program and variations in the frequency of efficiencies $eta_{21\_f\_ss}$, $eta_{21\_S21\_f\_ss}$ and $eta_{12\_S12\_f\_ss}$; c)Calculated with programs SCAP and SYSEG; d)$eta_{21\_S21\_f\_ss}$ and $eta_{12\_S12\_f\_ss}$ calculated with ADS, g = 250 mm, M_{Q3D} = 0.64191 µH, k_{Q3D}= 0.03834.

(a)
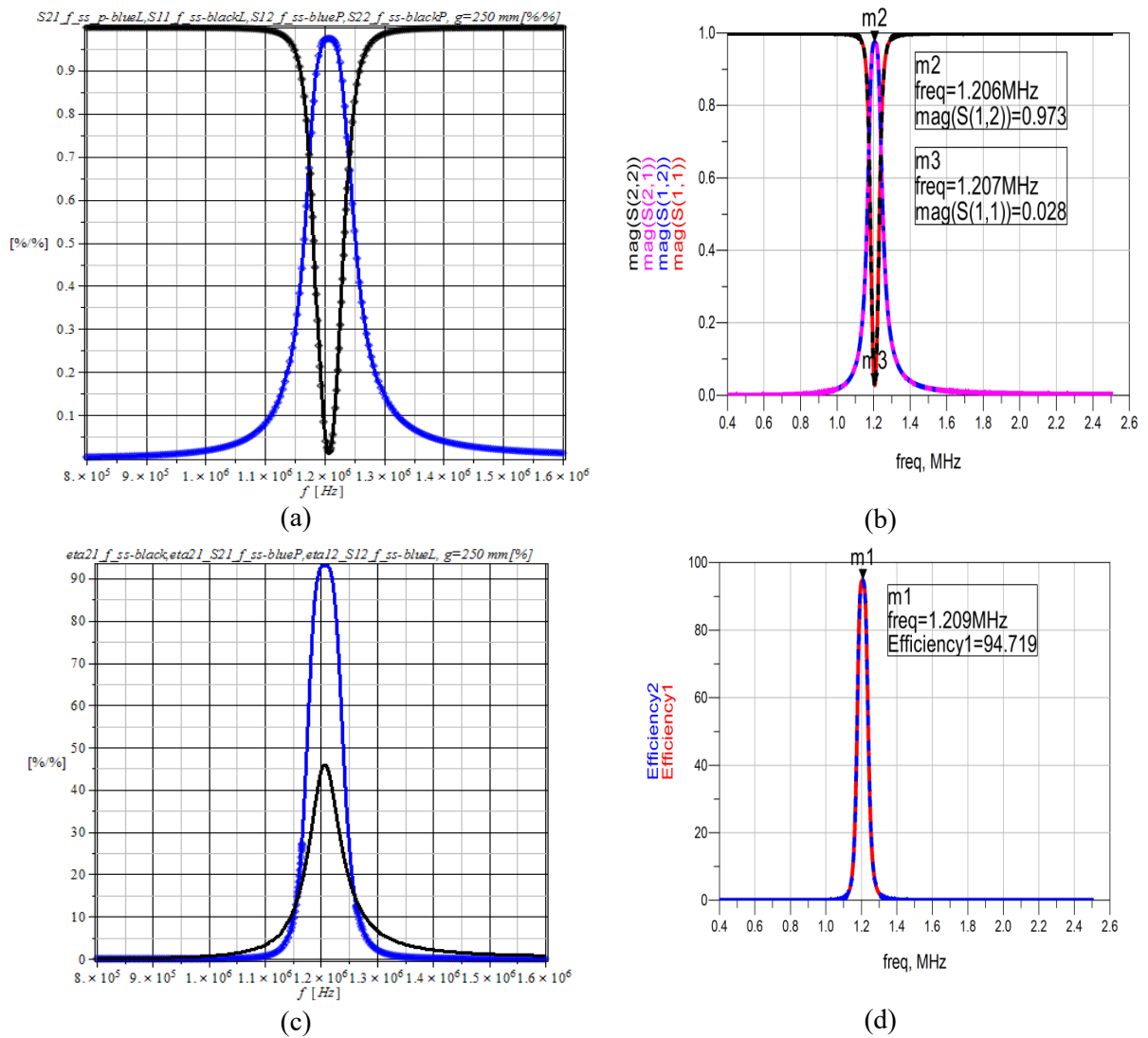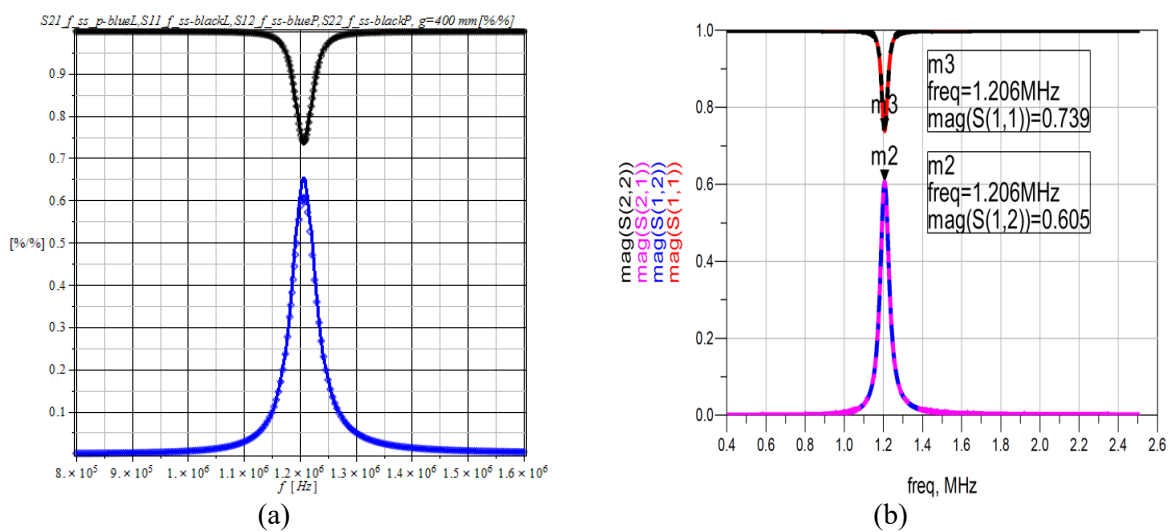

(b)

(c)   (d)

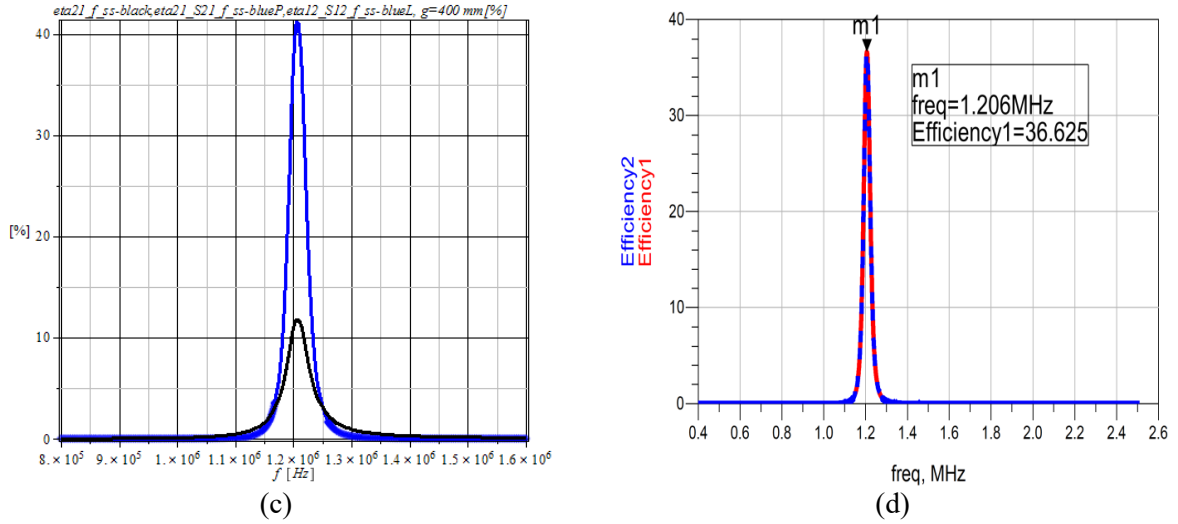**Fig. 2.15.** Variations with the frequency of parameter modules $\underline{S}_{11\_f\_ss}$, $\underline{S}_{21\_f\_ss}$, $\underline{S}_{22\_f\_ss}$ and $\underline{S}_{12\_f\_ss}$: a)Calculated with programs SCAP and SYSEG; b)Calculated with ADS program and variations in the frequency of efficiencies $eta_{21\_f\_ss}$, $eta_{21\_S21\_f\_ss}$ and $eta_{12\_S12\_f\_ss}$; c)Calculated with programs SCAP and SYSEG; d)$eta_{21\_S21\_f\_ss}$ and $eta_{12\_S12\_f\_ss}$ calculated with ADS, $g = 400$ mm, $M_{Q3D} = 0.23558$ µH, $k_{Q3D} = 0.01407$.

2.5. Conclusions

In this chapter, using circuit theory, several particularly effective procedures for calculating $\underline{S}$ parameters were exposed, based on the state equations and the modified nodal equations. There were also presented the practical way of using the parameters in streamlining the processes of information transmission and propagation and the wireless transfer of electromagnetic energy from the point of view of signal transmission and power from the transmitter to the receiver. The procedures for calculating the $\underline{S}$ parameters use the most advanced calculation programs, such as CADENCE [13, 14, 24], ADS [17, 21, 22, 26], ANSYS și ANSOFT EXTRACTOR Q3D [19, 25, 29], FEKO [20] etc.

The correct definition, based on the theory of electrical circuits, of $\underline{S}$ parameters allowed their automatic generation, using the state equations or the modified nodal equations.

Considering the two magnetically coupled coils (resonators) used in wireless power transfer as a passive linear two-port circuit in harmonic mode, the $\underline{S}$ parameters for all types of connections are determined. The paper shows the practical way of using these parameters in the efficiency of the processes of transmission and propagation of information and of the wireless transfer of electromagnetic energy from the transmitter to the receiver.

The passive linear two-port circuit by which the system consisting of two magnetically coupled coils can be equivaled allows the calculation of the maximum active power supplied to the load.

Comparing the variations with the frequency of the active power transmission efficiencies η_{21} and η_{12} with those of signal transmission η_{21_S21} and η_{12_S12}, it is found that the frequencies corresponding to the extreme points are not identical. The active power transmission efficiencies have a single maximum, while the signal transmission efficiencies have two maximums, appearing, in this case, the phenomenon of frequency splitting.

Figures 2.13 to 2.15 shows that the results obtained with the three SCAP, SYSEG and ADS programs are identical, which confirms the validity of the formulas (2.3) – (2.6) and of the proposed calculation procedures.

The accuracy of $\underline{S}$ parameters definition, based on the theory of analog circuits in harmonic regime, in complex, the relations (2.3) – (2.6), is confirmed by the results obtained with the ADS program, that has specific subroutines for the generation of $\underline{S}$ parameters.

3. THE USE OF $\underline{S}$ PARAMETERS IN THE ANALYSIS OF TWO-PORT CIRCUITS

3.1. Introduction

In the analysis of linear devices in harmonic mode, at low frequencies the matrices of the transfer coefficients and those of the impedances or admittances are usually used, but in the microwave field, where the frequencies are high, they are difficult to be measured and as a result at these high frequencies scattering parameters $\underline{S}$ are preferred.

In chapter 2, using electrical circuit theory and the correct definition of $\underline{S}$ parameters, it was automatically generated, through several procedures, the $\underline{\boldsymbol{S}}$ matrix of scattering parameters. In this chapter, based on this matrix, the calculation of the $\underline{\boldsymbol{Z}}$, $\underline{\boldsymbol{Y}}$ and $\boldsymbol{T}$ matrices is carried out.

Depending on $\underline{S}$ parameters, the parameters that characterize the analog filters are determined and the frequency bandwidths of the passage and stopping of the analyzed filters are calculated and obviously, implicitly, the nature of these filters is calculated.

At the end, routines were implemented, based on the elaborated procedures, in the MAPLE programming environment in order to calculate all the parameters mentioned above and to be able to compare the results obtained by simulation with those existing in the specialized literature and with the experimental ones.

3.2. The use of $\underline{S}$ parameters in the analysis of two-port electrical circuit systems

In this paragraph, using the theory of electrical circuits, there is presented, based on the matrix $\underline{\boldsymbol{S}}$ of $\underline{S}$ parameters, the calculation of matrices $\underline{\boldsymbol{Z}}$, $\underline{\boldsymbol{Y}}$ and $\underline{\boldsymbol{T}}$. In paragraph 3.2, for any type of linear or nonlinear two-port circuit – linearized on portions in the harmonic regime, there are determined as follows: the matrix of complex impedances $\underline{\boldsymbol{Z}}$, the matrix of complex admittances $\underline{\boldsymbol{Y}}$, the matrix of complex transfer coefficients (fundamental) $\underline{\boldsymbol{T}}$, the complex input and output impedances, $\underline{Z}_{in}$ and $\underline{Z}_{out}$, the coefficients of reflection from the generator Γ_G, from the load Γ_L, from the input Γ_{in} and from the output Γ_{out}, the equivalent voltage generator (Thévenin equivalent circuit) in relation to the output port of the two-port circuit and there are deduced the relationships between these dimensions and the $\underline{S}$ parameters. There is exposed the practical way of using these parameters in the efficiency of transmission and propagation of information processes and of the transfer of electromagnetic energy from the point of view of signal transmission from the input to the output of two-port circuits and from the point of view of the efficiency of the transfer of the active power from the input of the two-port circuits to the loads connected to their output. Based on the theorem of the maximum active power transfer, there is calculated the maximum active power transmitted by a circuit to the load.

The generation of $\underline{S}$ parameters for linear analogue circuits and for nonlinear analog circuits, linearized on portions around a point of operation, under precise polarization and temperature conditions of electronic devices, can be carried out by means of small signal simulations, [1].

For the generation of $\underline{S}$ parameters for nonlinear circuits, the LSSP – Large-Signal S-Parameter Simulation simulator [18] is used, which uses the method of analyzing the *harmonic balance*. Simulation based on the harmonic balance method is a *large signal* simulation, to which solutions also include the effects of nonlinearities of electronic components. $\underline{S}$ parameters, both small and large signals, are defined as ratios between incident and reflected waves, [4, 8].

The following relations can be easily demonstrated:

$$\underline{Z} = \left(I_2 - \underline{S}\right)^{-1} \cdot \left(I_2 + \underline{S}\right) Z_0, \tag{3.1}$$

where I_2 is the unit matrix of order 2;

$$\underline{S} = \left(\underline{Z} - Z_0 I_2\right) \cdot \left(\underline{Z} + Z_0 I_2\right)^{-1}; \tag{3.2}$$

$$\underline{T} = \frac{1}{\underline{Z}_{21}} \begin{bmatrix} \underline{Z}_{11} & -\underline{Z}_{11} \cdot \underline{Z}_{22} + \underline{Z}_{12} \cdot \underline{Z}_{21} \\ 1 & -\underline{Z}_{22} \end{bmatrix}; \tag{3.3}$$

$$\underline{Z} = \frac{1}{\underline{C}} \begin{bmatrix} \underline{A} & -\underline{A} \cdot \underline{D} + \underline{B} \cdot \underline{C} \\ 1 & -\underline{D} \end{bmatrix}; \tag{3.4}$$

$$\underline{Y} = \frac{1}{\underline{Z}_{11}\underline{Z}_{22} - \underline{Z}_{12}\underline{Z}_{21}} \begin{bmatrix} \underline{Z}_{22} & -\underline{Z}_{12} \\ -\underline{Z}_{21} & \underline{Z}_{11} \end{bmatrix}. \tag{3.5}$$

For the definition of complex input and output impedances and reflection coefficients Γ_{in} (input), Γ_{out} (output), Γ_G (from generator) and Γ_L (from load), the system consisting of two magnetically coupled coils, used in the wireless transfer of electromagnetic power, can be equivaled with the passive linear two-port circuit (in the harmonic mode) represented in Figure 3.1, [1, 4, 5, 6, 8, 10, 11, 15, 16].
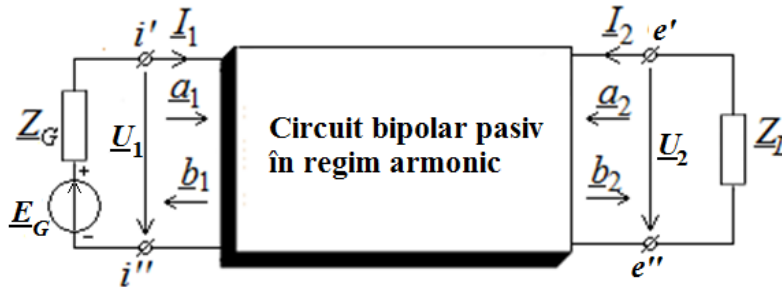
Fig. 3.1. Passive linear two-port circuit connected to the generator and load.

Starting from the relations that define the two-port circuit from Fig. 3.1. the following can be demonstrated:

$$\underline{Z}_{in} = \underline{Z}_{11} - \frac{\underline{Z}_{12}\underline{Z}_{21}}{\underline{Z}_L + \underline{Z}_{22}}, \tag{3.6}$$

$$\underline{Z}_{out} = \underline{Z}_{22} - \frac{\underline{Z}_{12}\underline{Z}_{21}}{\underline{Z}_G + \underline{Z}_{11}}. \tag{3.7}$$

$$\underline{\Gamma}_{in} = \frac{b_1}{a_1}\bigg|_{\substack{E_G=0, U_1=\underline{Z}_{in}I_1 \\ U_2=-\underline{Z}_L I_2}} = \frac{\left(\underline{Z}_{in}\underline{I}_1 - Z_0\underline{I}_1\right)/2\sqrt{Z_0}}{\left(\underline{Z}_{in}\underline{I}_1 + Z_0\underline{I}_1\right)/2\sqrt{Z_0}} = \frac{\underline{Z}_{in} - Z_0}{\underline{Z}_{in} + Z_0} \Rightarrow \underline{Z}_{in} = Z_0\frac{1+\underline{\Gamma}_{in}}{1-\underline{\Gamma}_{in}}. \tag{3.8}$$

$$\Gamma_G = \frac{(-\underline{Z}_G \underline{I}_1 + Z_0 \underline{I}_1)/2\sqrt{Z_0}}{(-\underline{Z}_G \underline{I}_1 - Z_0 \underline{I}_1)/2\sqrt{Z_0}} = \frac{\underline{Z}_G - Z_0}{\underline{Z}_G + Z_0} \Rightarrow \underline{Z}_G = Z_0 \frac{1 + \Gamma_G}{1 - \Gamma_G}. \tag{3.9}$$

$$\Gamma_{out} = \frac{b_2}{a_2}\bigg|_{\substack{E_G=0, U_1 = Z_{in} I_1 \\ U_2 = Z_{out} I_2}} = \frac{(\underline{Z}_{out} \underline{I}_2 - Z_0 \underline{I}_2)/2\sqrt{Z_0}}{(\underline{Z}_{out} \underline{I}_2 + Z_0 \underline{I}_2)/2\sqrt{Z_0}} = \frac{\underline{Z}_{out} - Z_0}{\underline{Z}_{out} + Z_0} \Rightarrow \underline{Z}_{out} = Z_0 \frac{1 + \Gamma_{out}}{1 - \Gamma_{out}}. \tag{3.10}$$

$$\Gamma_L = \frac{(-\underline{Z}_L \underline{I}_2 + Z_0 \underline{I}_2)/2\sqrt{Z_0}}{(-\underline{Z}_L \underline{I}_2 - Z_0 \underline{I}_2)/2\sqrt{Z_0}} = \frac{\underline{Z}_L - Z_0}{\underline{Z}_L + Z_0} \Rightarrow \underline{Z}_L = Z_0 \frac{1 + \Gamma_L}{1 - \Gamma_L}. \tag{3.11}$$

Starting from the definition of $\underline{S}$ parameters according to the incident and reflected signals, after a few simple calculations, these expressions can be defined:

$$\Gamma_{in} = \underline{S}_{11} + \frac{\underline{S}_{12}\underline{S}_{21}\Gamma_L}{1 - \underline{S}_{22}\Gamma_L} \text{ and } \Gamma_{out} = \underline{S}_{22} + \frac{\underline{S}_{12}\underline{S}_{21}\Gamma_G}{1 - \underline{S}_{11}\Gamma_G}. \tag{3.12}$$

The input and output impedances $\underline{Z}_{in}$ and $\underline{Z}_{out}$ allow the substitution, according to the theorem of the equivalent voltage generator (Thévenin's theorem), of the passive linear two-port circuit from figure 3.1 with the equivalent circuits represented in figure 3.2, [31].
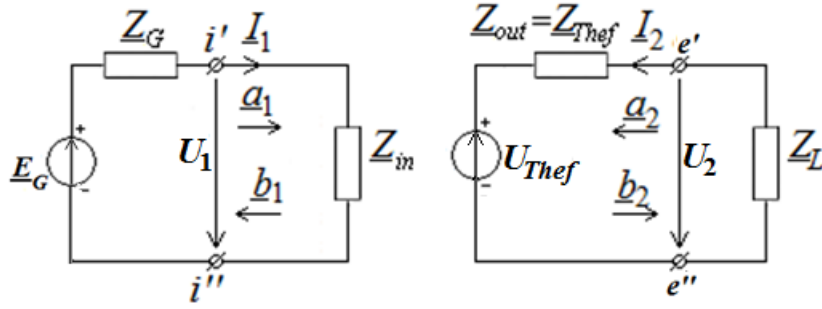

Fig. 3.2. Equivalent circuits at the input and output of a passive linear two-port circuit in harmonic mode.

The voltage $\underline{U}_{Thef} = \underline{U}_2\big|_{\underline{I}_2=0, \underline{U}_1 = \underline{E}_G - \underline{Z}_G \underline{I}_1} = \frac{\underline{Z}_{21}}{\underline{Z}_G + \underline{Z}_{11}} \underline{E}_G$, and $\underline{Z}_{Thef} = \frac{\underline{U}_{Thef}}{\underline{I}_{2\_0}} = \underline{Z}_{out}$.

The system consisting of the two magnetically coupled resonators used in the wireless transfer of electromagnetic power can be considered as a passive linear two-port circuit represented in figure 3.1.

The active power supplied to the output port has the expression:

$$P_2 = P_L = -\operatorname{Re}\left(\underline{V}_2 \cdot \underline{I}_2^*\right) = -|a_2|^2 + |b_2|^2. \tag{3.13}$$

Power losses are as follows:

$$P_{loss} = P_1 - P_2 = |a_1|^2 + |a_2|^2 - |b_1|^2 - |b_2|^2 = \left(\underline{a}^*\right)^t \cdot \underline{a} - \left(\underline{b}^*\right)^t \cdot \underline{b}. \tag{3.14}$$

If we consider that $\underline{b} = \underline{S}^*\underline{a}$, the efficiency of transmission of active power from the transmitting coil to the load can be calculated with the relations:

$$\eta_{21} = \frac{P_2}{P_1} \cdot 100 = \frac{R_L}{R_{in}} \cdot \left|\frac{\underline{Z}_{21}}{\underline{Z}_{22} + \underline{Z}_L}\right|^2 \cdot 100 = \frac{|\underline{S}_{21}|^2 \cdot \left(1 - |\Gamma_L|^2\right)}{\left(1 - \left|\left(1 - |\Gamma_L|^2\right)\right|^2\right) \cdot |1 - \underline{S}_{22}\Gamma_L|^2} \cdot 100, \tag{3.15}$$

where $R_{in} = \operatorname{Re}(\underline{Z}_{in})$ and $R_L = \operatorname{Re}(\underline{Z}_L)$.

The efficiency of transmission of signals from the input to the load has the expression: $\tag{3.16}$

$$\eta_{21\_S_{21}} = \underline{S}_{21} \cdot \underline{S}_{21}^* \cdot 100 = \left|\underline{S}_{21}\right|^2 \cdot 100,$$

And the efficiency of transmitting signals from the output to the generator is calculated with the relation:

$$\eta_{12\_S_{12}} = \underline{S}_{12} \cdot \underline{S}_{12}^* \cdot 100 = \left|\underline{S}_{12}\right|^2 \cdot 100. \tag{3.17}$$

According to the theorem of the maximum power transfer, the load receives maximum power if $\underline{Z}_L = Z^*_{out}$ and it has the expression:

$$P_{L\_max} = \frac{V_{Thef}^2}{4 \cdot \mathrm{Re}\left(\underline{Z}_{out}\right)}. \tag{3.18}$$

The equations of a passive linear quadrupole (fig. 3.3) in the fundamental (transfer) parameters have the form:

$$\begin{bmatrix} \underline{U}_1 \\ \underline{I}_1 \end{bmatrix} = \begin{bmatrix} \underline{A} & \underline{B} \\ \underline{C} & \underline{D} \end{bmatrix} \begin{bmatrix} \underline{U}_2 \\ \underline{I}_2 \end{bmatrix}. \tag{3.19}$$
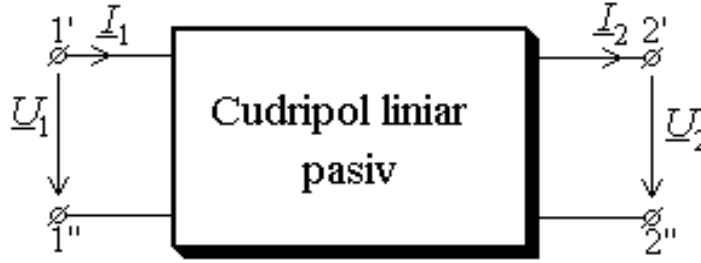

Fig. 3.3. The scheme of the passive linear quadrupole.

Fundamental parameters have, by definition, expressions:

$$\underline{A} \overset{d}{=} \left.\frac{\underline{U}_1}{\underline{U}_2}\right|_{I_2=0} = \frac{1}{\underline{A}_{ei}}; \quad \underline{B} \overset{d}{=} \left.\frac{\underline{U}_1}{\underline{I}_2}\right|_{U_2=0} = \frac{1}{\underline{Y}_{ei}};$$

$$\underline{C} \overset{d}{=} \left.\frac{\underline{I}_1}{\underline{U}_2}\right|_{I_2=0} = \frac{1}{\underline{Z}_{ei}}; \quad \underline{D} \overset{d}{=} \left.\frac{\underline{I}_1}{\underline{I}_2}\right|_{U_2=0} = \frac{1}{\underline{B}_{ei}} \tag{3.20}$$

Impedance equations of a passive linear quadrupole have the expressions:

$$\begin{bmatrix} \underline{U}_1 \\ \underline{U}_2 \end{bmatrix} = \begin{bmatrix} \underline{Z}_{11} & \underline{Z}_{12} \\ \underline{Z}_{21} & \underline{Z}_{22} \end{bmatrix} \begin{bmatrix} \underline{I}_1 \\ \underline{I}_2 \end{bmatrix}, \tag{3.21}$$

where complex transfer impedances are defined as follows:

$$\underline{Z}_{11} \overset{d}{=} \left.\frac{\underline{U}_1}{\underline{I}_1}\right|_{I_2=0} = \underline{Z}_{ii}; \quad \underline{Z}_{12} \overset{d}{=} \left.\frac{\underline{U}_1}{\underline{I}_2}\right|_{I_1=0} = -\underline{Z}_{ie};$$

$$\underline{Z}_{21} \overset{d}{=} \left.\frac{\underline{U}_2}{\underline{I}_1}\right|_{I_2=0} = \underline{Z}_{ei}; \quad \underline{Z}_{22} \overset{d}{=} \left.\frac{\underline{U}_2}{\underline{I}_2}\right|_{I_1=0} = -\underline{Z}_{ee}. \tag{3.22}$$

The equations in admittances of a passive linear quadrupole have the form:

$$\begin{bmatrix} \underline{I}_1 \\ \underline{I}_2 \end{bmatrix} = \begin{bmatrix} \underline{Y}_{11} & \underline{Y}_{12} \\ \underline{Y}_{21} & \underline{Y}_{22} \end{bmatrix} \begin{bmatrix} \underline{U}_1 \\ \underline{U}_2 \end{bmatrix}, \tag{3.23}$$

where the complex transfer admittances are defined as follows:

$$\underline{Y}_{11} = \frac{\mathrm{d}\,\underline{I}_1}{\underline{U}_1}\bigg|_{\underline{U}_2=0} = \underline{Y}_{ii}; \quad \underline{Y}_{12} = \frac{\mathrm{d}\,\underline{I}_1}{\underline{U}_2}\bigg|_{\underline{U}_1=0} = -\underline{Y}_{ie};$$

$$\underline{Y}_{21} = \frac{\mathrm{d}\,\underline{I}_2}{\underline{U}_1}\bigg|_{\underline{U}_2=0} = \underline{Y}_{ei}; \quad \underline{Y}_{22} = \frac{\mathrm{d}\,\underline{I}_2}{\underline{U}_2}\bigg|_{\underline{U}_1=0} = -\underline{Y}_{ee}.$$

(3.24)

The characteristic impedances of a passive linear quadrupole are defined as follows:

$$\underline{Z}_{c1} = \frac{\mathrm{d}\,\underline{U}_1}{\underline{I}_1}\bigg|_{\underline{Z}_s=\underline{Z}_{c1}}; \quad \underline{Z}_{c2} = \frac{\mathrm{d}\,\underline{U}_2}{-\underline{I}_2}\bigg|_{\underline{Z}_i=\underline{Z}_{c2}}, \tag{3.25}$$

and the two images have the expressions:

$$\underline{Z}_{i1} = \frac{\mathrm{d}\,\underline{U}_1}{\underline{I}_1}\bigg|_{\underline{Z}_s=\underline{Z}_{i2}}; \quad \underline{Z}_{i2} = \frac{\mathrm{d}\,\underline{U}_2}{-\underline{I}_2}\bigg|_{\underline{Z}_i=\underline{Z}_{i1}}. \tag{3.26}$$

The expressions of the characteristic impedances according to the fundamental (transfer) parameters of the quadrupole are as follows:

$$\underline{Z}_{c1} = \frac{1}{2\underline{C}}\left[(\underline{A}-\underline{D}) \pm \sqrt{(\underline{A}-\underline{D})^2 + 4\underline{B}\underline{C}}\right],$$

$$\underline{Z}_{c2} = \frac{1}{2\underline{C}}\left[(\underline{D}-\underline{A}) \pm \sqrt{(\underline{D}-\underline{A})^2 + 4\underline{B}\underline{C}}\right].$$

(3.27)

The image impedances, expressed according to the fundamental (transfer) parameters of the quadrupole, have the expressions:

$$\underline{Z}_{i1} = \pm\sqrt{\frac{\underline{A}\underline{B}}{\underline{C}\underline{D}}}, \quad \underline{Z}_{i2} = \pm\sqrt{\frac{\underline{D}\underline{B}}{\underline{C}\underline{A}}}. \tag{3.28}$$

If the quadrupole is symmetrical, the equations (3.27) and (3.28) become:

$$\underline{Z}_{c1} = \underline{Z}_{c2} = \underline{Z}_{i1} = \underline{Z}_{i2} = \pm\sqrt{\frac{\underline{B}}{\underline{C}}}. \tag{3.29}$$

The transfer factors on the characteristic and, respectively, on the image impedances, depending on the transfer parameters, are given by the relations:

$$\underline{\gamma}_c = \ln\left(\frac{1}{2}\left[(\underline{A}+\underline{D}) + \sqrt{(\underline{A}+\underline{D})^2 - 4}\right]\right),$$

$$\underline{\gamma}_i = \ln\left(\sqrt{\underline{A}\underline{D}} + \sqrt{\underline{B}\underline{C}}\right).$$

(3.30)

If the quadrupole is symmetrical, the equations (3.30) become:

$$\underline{\gamma}_c = \underline{\gamma}_i = \ln\left(\underline{A} + \sqrt{\underline{B}\underline{C}}\right). \tag{3.31}$$

In the case of reciprocal and lossless filters, the passing (stopping) intervals are made up of all the frequencies for which the inecuation is (is not) satisfied:

$$0 \le AD \le 1. \tag{3.32}$$

Attenuation constant a and phase constant b have, in filter passing intervals, the following expressions:

$$a = 0, \quad b = arcctg\,\frac{1}{\sqrt{\frac{1}{AD} - 1}} + k\pi = \arccos\sqrt{AD} + k\pi, \tag{3.33}$$

and in the stopping intervals these quantities are given by the expressions:

$$a = \arg cth \frac{1}{\sqrt{1 - \dfrac{1}{AD}}} = \operatorname{argch}\sqrt{AD}, \quad b = \begin{cases} \pm \dfrac{\pi}{2} & AD \leq 0 \\ 0 \text{ sau } 1 & AD \geq 1 \end{cases}.$$ (3.34)

Three widely used definitions for the power gain of a two-port circuit are: *the captured power gain G_t, the available power gain G_a* and *the gain (efficiency) of power transfer G_p*, also called the *operating gain*.

These gains can be expressed according to the parameters $\underline{S}$, $\underline{Z}$ and the coefficients of reflection, as follows:

$$G_t = \frac{\text{power out of network}}{\text{maximum power in}} = \frac{1 - |\Gamma_G|^2}{|1 - \Gamma_{in}\Gamma_G|^2} |S_{21}|^2 \frac{1 - |\Gamma_L|^2}{|1 - \underline{S}_{22}\Gamma_L|^2} =$$

$$= \frac{1 - |\Gamma_L|^2}{|1 - \Gamma_{out}\Gamma_L|^2} |S_{21}|^2 \frac{1 - |\Gamma_G|^2}{|1 - \underline{S}_{11}\Gamma_G|^2}$$ (3.35)

$$G_a = \frac{\text{maximum power out}}{\text{maximum power in}} = \frac{R_G}{R_{out}} \left| \frac{\underline{Z}_{21}}{\underline{Z}_{11} + \underline{Z}_G} \right|^2 = \frac{1 - |\Gamma_G|^2}{|1 - \underline{S}_{11}\Gamma_G|^2} |S_{21}|^2 \frac{1}{1 - |\Gamma_{out}|^2},$$ (3.36)

and

$$G_p = \eta_{21} = \frac{\text{power out of network}}{\text{power into power}} \cdot 100 = \frac{R_L}{R_{in}} \left| \frac{\underline{Z}_{21}}{\underline{Z}_{11} + \underline{Z}_G} \right|^2 =$$

$$= \frac{1}{1 - |\Gamma_{in}|^2} |S_{21}|^2 \frac{1 - |\Gamma_L|^2}{|1 - \underline{S}_{22}\Gamma_L|^2} \cdot 100$$ (3.37)

3.3. Example

The low-pass filter represented in figure 3.4 will be studied using the ASINOM symbolic simulator.
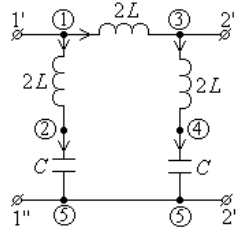

Fig. 3.4. Structure of the non-dissipative low-pass filter.

First, the $\underline{S}$ parameters are generated for the filter from figure 3.4.

After generating the $\underline{S}$ parameters, the matrix of the complex impedances $\underline{Z}$ is calculated with the relation (3.1), and then all the desired parameters of the filter are determined.

The $\underline{T}$ matrix of the fundamental (transfer) parameters has the following form:

$$T := \begin{bmatrix} \dfrac{4.\,\omega^2\,C\,L - 1.}{-1. + 2.\,\omega^2\,C\,L} & -2.\,I\,\omega\,L \\ \dfrac{-2.\,I\,\omega\,C\,(3.\,\omega^2\,C\,L - 1.)}{1. - 4.\,\omega^2\,C\,L + 4.\,\omega^4\,C^2\,L^2} & -\dfrac{1.\,(4.\,\omega^2\,C\,L - 1.)}{-1. + 2.\,\omega^2\,C\,L} \end{bmatrix}$$ (3.38)

For the numerical values $L = 1\,\text{mH}$ and $C = 2\ \mu\text{F}$, with the formula (3.32), there are calculated the passing and stopping bandwidths of the filter and implicitly its nature:

$$\omega \in \left[0,\ 12909.944\right] \text{ - passing bandwidth and}$$

$$\omega \in \left(12909.944,\ \infty\right) \text{ - stopping bandwidth.}$$

(3.39)

So, the filter represented in figure 3.4 is a low-pass filter.

The transfer (amplification) factor has, depending on the frequency, the expression:

$$Aoi\_f := \frac{0.5000\,(-0.2500\ 10^9 + 39.44\,f^2)}{39.44\,f^2 - 0.1250\ 10^9}.$$

(3.40)

In figure 3.5, a (fig. 3.5, b) the frequency variation of the amplitude (phase) of the transfer (amplification) factor in voltage A_{oi} is shown.
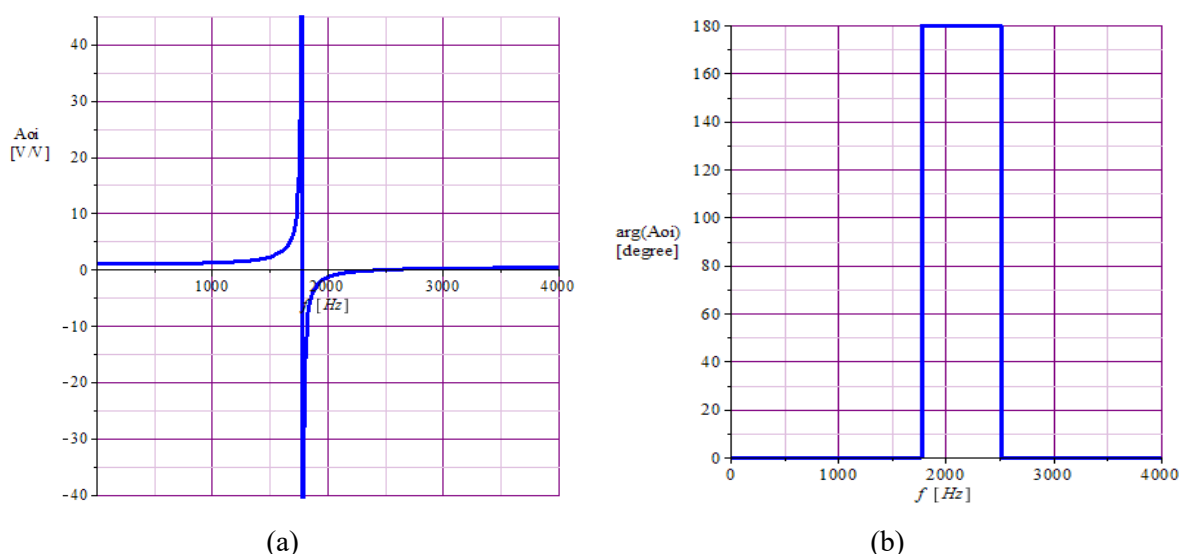

(a)   (b)

Fig. 3.5. a) Variation with the frequency of the magnitude abs(A_{oi_f}); b) Variation with the frequency of the argument arg(A_{oi_f}).

Variations with pulsation ω of attenuation factor a and phase constant b are shown in figures 3.6, a and 3.6, b respectively.

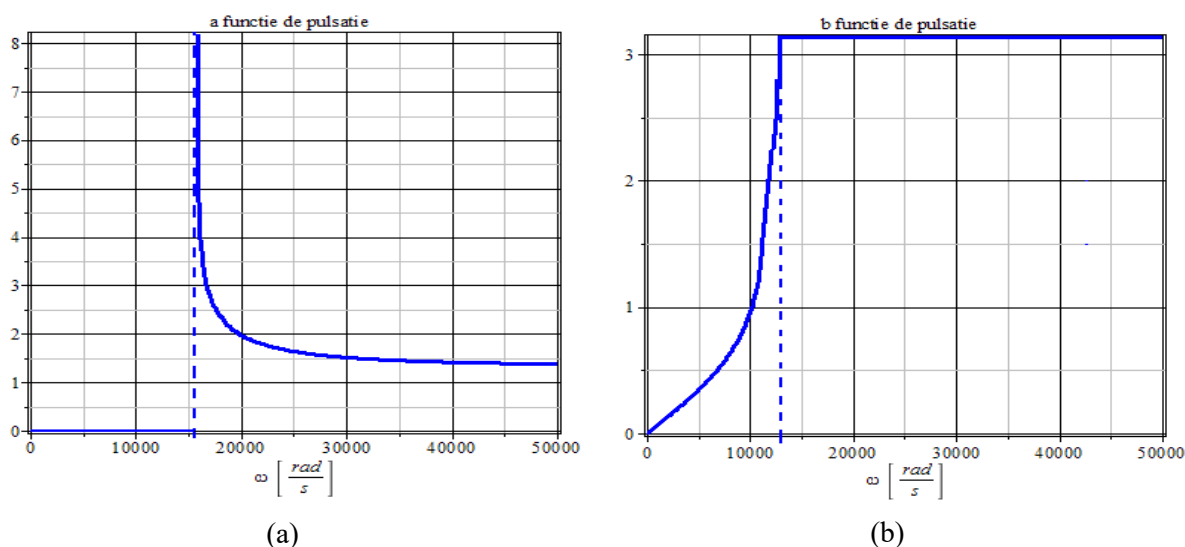(a)   (b)

Fig. 3.6. a) Variation with pulsation of the attenuation constant a; b) Variation with pulsation of the phase constant b.

In order to be able to use the ADS program for the filter analysis from figure 3.4, the diagram in figure 3.7 was developed [17].
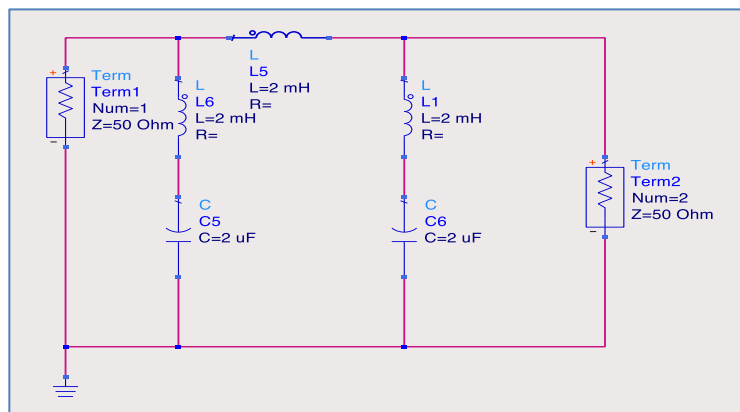
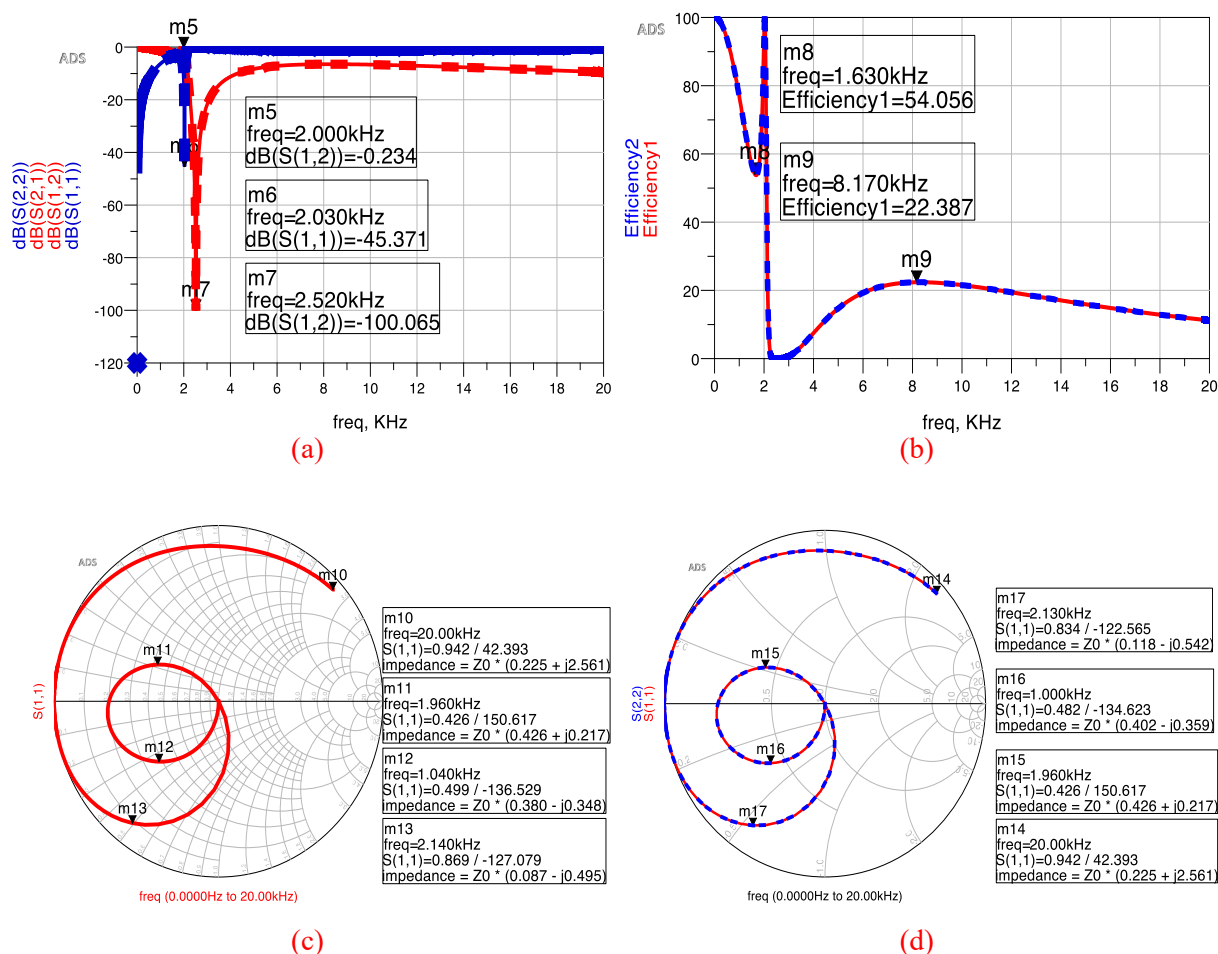**Fig. 3.7.** Schema filtrului din figura 3.4 utilizată de programul ADS.

(a)

(b)

(c)

(d)

Fig. 3.8. Charts obtained with the ADS program: a) Variations with the frequency of magnitudes for $\underline{S}_{11}$, $\underline{S}_{12}$, $\underline{S}_{21}$ and $\underline{S}_{22}$; b) Variations in frequency of signal transmission efficiencies η_{21_S21} and η_{12_S12}; c) Chart of the parameter $\underline{S}_{11}$, identical (due to symmetry) with $\underline{S}_{22}$, on Smith diagram; d) Charts of parameters $\underline{S}_{12}$ and $\underline{S}_{21}$, identical (due to symmetry) on Smith diagram.

Figures 3.8, a, b, c and d represent the charts obtained from running the ADS program for the circuit from figure 3.7, as follows: a) Variations with the frequency of magnitudes for $\underline{S}_{11}$, $\underline{S}_{12}$, $\underline{S}_{21}$ and $\underline{S}_{22}$; b) Variations in frequency of signal transmission efficiencies η_{21_S21} and η_{12_S12}; c) Chart of the parameter $\underline{S}_{11}$, identical (due to symmetry) with $\underline{S}_{22}$, on Smith diagram; d) Charts of parameters $\underline{S}_{12}$ and $\underline{S}_{21}$, identical (due to symmetry) on Smith diagram.

In the figures 3.8, a, b, c and d are marked the representative points for each curve.

24

3.4. Conclusions

The correct definition, based on the theory of electrical circuits, of $\underline{S}$ parameters allowed their automatic generation, using the state equations or the modified nodal equations. Once the $\underline{S}$ parameters have been generated, for a set of frequencies, there can be generated: $\underline{\mathbf{T}}$, $\underline{\mathbf{Z}}$ and $\underline{\mathbf{Y}}$ matrices; $\underline{\Gamma}_G$, $\underline{\Gamma}_L$, $\underline{\Gamma}_{in}$ and $\underline{\Gamma}_{out}$ reflection coefficients; active power transmission efficiencies η_{21} and η_{12}; signal transmission efficiencies η_{21_S21} and η_{12_S12}; input and output impedances $\underline{Z}_{in}$ and $\underline{Z}_{out}$; Thévenin equivalent generator; the captured power gain G_t, available power gain G_a and the gain (efficiency) of power transfer G_p, also called the operating gain and Smith diagrams for $\underline{S}$ parameters.

Considering the two coupled oscillators, as a passive linear two-port circuit in the harmonic regime, all the parameters mentioned above are determined, according to $\underline{S}$ parameters. The paper shows the practical way of using these parameters in the efficiency of the information transmission and propagation processes and of the transfer of the active power from input (output) to output (input).

Comparing variations with the frequency of the active power transmission efficiency η_{21} with those ones of the signal transmission η_{21_S21} și η_{12_S12} there is learned that the frequencies corresponding to the extreme points are identical. All the efficiencies have two maximums, appearing, in this case, the phenomenon of splitting the frequency. Due to the symmetry, the variations with the frequency of the signal transmission efficiencies η_{21_S21} and η_{12_S12} are identical.

The passive linear two-port circuit by which the system consisting of two coupled Van der Poll oscillators can be equivaled allows the calculation of the maximum active power supplied to the load. From a mathematical point of view, the Smith diagram is a 4D representation of all possible complex impedances in relation to the coordinates defined by the complex coefficient of reflection, for any desired frequency.

The accuracy of defining the $\underline{S}$ parameters, based on the theory of analog circuits in the harmonic regime in complex, the relations (2.6) – (2.9), is confirmed by the results obtained with the ADS program, endowed with specific subroutines for the generation of $\underline{S}$ parameters.

4. THE USE OF $\underline{S}$ PARAMETERS IN THE STABILITY OF WIRELESS ELECTROMAGNETIC ENERGY TRANSFER SYSTEMS

4.1. Introduction

Considering the system consisting of two magnetically coupled coils, used in the wireless transfer of the electromagnetic energy, as a linear two-port circuit in the harmonic regime, there is described the possibility of using $\underline{S}$ parameters in determining the stable operating regions of these coils.

The two magnetically coupled coils, considered as a passive linear two-port circuit in the harmonic regime, can be described by several equivalent circuit parameters, such as: the matrix of the transfer (fundamental) T, the matrix of the Z impedances, the matrix of the admittances $\underline{Y}$ and the matrix of the parameters $\underline{S}$. In literature, [8, 14, 15], there are procedures that allow the transition from one matrix to another.

Using the theory of electrical circuits, it is presented, starting from the correct definition of the $\underline{S}$ parameters (based on the theory of circuits) [10], the automatic generation of the matrix $\underline{S}$ of the scattering parameters, and then, based on this matrix, the calculation of the $\underline{Z}$, $\underline{Y}$ and $\underline{T}$ matrices. In paragraph 4.2, considering the two magnetically coupled coils used in the wireless transfer of power [20 – 24], as a passive linear two-port circuit in harmonic mode, it is determined: complex input and output impedances, $\underline{Z}_{in}$ and $\underline{Z}_{out}$ the coefficients of reflection from the generator $\underline{\Gamma}_G$, from the load $\underline{\Gamma}_L$, from the input $\underline{\Gamma}_{in}$ and from the output $\underline{\Gamma}_{out}$, the desired transfer functions and the relationships between these sizes and the $\underline{S}$ parameters are deduced. There is exposed the practical way of using these parameters in streamlining the processes of transmission and propagation of information and the wireless transfer of electromagnetic energy from the point of view of transmission of signals from the transmitter to the receiver and from the point of view of the efficiency of the transfer of the active power from the input of the wireless systems to the loads connected to their output. Also, depending on $\underline{S}$ parameters, the most used coefficients of performance are determined in practice: the captured power gain G_t, the available power gain G_a, the gain (efficiency) of the transfer of the power G_p, also called the operating gain, the available power gain maximum G_{MAG}, and the power maximum stable gain G_{MSG} [11, 34 - 37].

At the end, procedures have been developed and implemented for the calculation of reflection coefficients, stationary wave ratios (SWR), input and output impedances, outputs of active power transmission from input to output (output to input), signal transmission efficiencies, power gains, various stability coefficients, centers and radii of the stability circles at the source and from the generator, the transfer functions, the $\underline{S}$, $\underline{T}$, $\underline{Z}$ and $\underline{Y}$ matrices, and the Smith diagrams. For the calculation of these parameters, dedicated functions and routines were developed in MATLAB and the existing routines from the Microwave toolbox in MATLAB were used. The results obtained by simulations were compared with those presented in the literature and with the experimental ones.

4.2. Stability of wireless power transfer systems

In discussions on the conditions of stability of a two-port circuit, depending on $\underline{S}$ parameters, the following definitions and constants are often used:

$$\underline{\Delta} = \det(\underline{S}) = \underline{S}_{11}\underline{S}_{22} - \underline{S}_{12}\underline{S}_{21} \; ; \; K = \frac{1 - \left|\underline{S}_{11}\right|^2 - \left|\underline{S}_{22}\right|^2 + \left|\underline{\Delta}_{11}\right|^2}{2\left|\underline{S}_{12}\underline{S}_{21}\right|} \text{Rollett stability factor;}$$

$$\begin{cases} \mu_1 = \dfrac{1 - \left|\underline{S}_{11}\right|^2}{\left|\underline{S}_{22} - \underline{\Delta}_{11}\underline{S}_{11}^*\right| + \left|\underline{S}_{12}\underline{S}_{21}\right|} \\[4mm] \mu_2 = \dfrac{1 - \left|\underline{S}_{22}\right|^2}{\left|\underline{S}_{11} - \underline{\Delta}_{11}\underline{S}_{22}^*\right| + \left|\underline{S}_{12}\underline{S}_{21}\right|} \end{cases} \Rightarrow \text{Edwards-Sinsky stability parameters;} \tag{4.1}$$

$$B_1 = 1 + \left|\underline{S}_{11}\right|^2 - \left|\underline{S}_{22}\right|^2 - \left|\underline{\Delta}\right|^2; \; B_2 = 1 + \left|\underline{S}_{22}\right|^2 - \left|\underline{S}_{11}\right|^2 - \left|\underline{\Delta}\right|^2;$$

$$\underline{C}_1 = \underline{S}_{11} - \underline{\Delta}\underline{S}_{22}^*; D_1 = \left|\underline{S}_{11}\right|^2 - \left|\underline{\Delta}\right|^2; \; \underline{C}_2 = \underline{S}_{22} - \underline{\Delta}\underline{S}_{11}^*; D_2 = \left|\underline{S}_{22}\right|^2 - \left|\underline{\Delta}\right|^2.$$

The centers and radii of the stability circles of the source (generator) and the load have the expressions:

$$\underline{c}_G = \frac{\underline{C}_1^*}{D_1}; \; r_G = \frac{\left|\underline{S}_{12}\underline{S}_{21}\right|}{\left|D_1\right|}; \; \underline{c}_L = \frac{\underline{C}_2^*}{D_2}; \; r_L = \frac{\left|\underline{S}_{12}\underline{S}_{21}\right|}{\left|D_2\right|} \tag{4.2}$$

Stability parameters μ_1 and μ_2 can also be calculated with relationships:

$$\mu_1 = \left(\left|\underline{c}_L\right| - r_L\right)sign(D_2); \; \mu_2 = \left(\left|\underline{c}_G\right| - r_G\right)sign(D_1). \tag{4.3}$$

Formulas can also be used to calculate the coefficients of reflection at the input and output:

$$\underline{\Gamma}_{in} = \underline{S}_{11} + \frac{\underline{S}_{12}\underline{S}_{21}\underline{\Gamma}_L}{1 - \underline{S}_{22}\underline{\Gamma}_L} = \frac{\underline{S}_{11} - \underline{\Delta}\underline{\Gamma}_L}{1 - \underline{S}_{22}\underline{\Gamma}_L};$$

$$\underline{\Gamma}_{out} = \underline{S}_{22} + \frac{\underline{S}_{12}\underline{S}_{21}\underline{\Gamma}_G}{1 - \underline{S}_{11}\underline{\Gamma}_G} = \frac{\underline{S}_{22} - \underline{\Delta}\underline{\Gamma}_G}{1 - \underline{S}_{11}\underline{\Gamma}_G}. \tag{4.4}$$

A two-port circuit is *unconditionally stable* if for any impedances of the generator and the load with the resistive (real) parts R_G and R_L positive always determine the input and output impedances with the resistive (real) parts R_{in} and R_{out} positive.

The load stability region is the set of all reflection coefficients $\underline{\Gamma}_L$ for which $|\underline{\Gamma}_{in}| < 1$, and the stability region of the generator is the set of all reflection coefficients $\underline{\Gamma}_G$ for which $|\underline{\Gamma}_{out}| < 1$. In the case of unconditional stability, the stability regions of the generator (source) and load contain the interiors of the unit circles with $|\underline{\Gamma}_L| < 1$ or $|\underline{\Gamma}_G| < 1$. However, in case of potential instability, only the portions of the unit circles can maintain stable regions and thus, $\underline{\Gamma}_G, \underline{\Gamma}_L$ will lead to stable output and input impedances.

The stability region of the load is defined as follows:

$$\left|\underline{\Gamma}_L - \underline{c}_L\right| > r_L, \text{ daca } D_2 > 0; \; \left|\underline{\Gamma}_L - \underline{c}_L\right| < r_L, \text{ daca } D_2 < 0, \tag{4.5}$$

The $\underline{\Gamma}_L - \underline{c}_L$ border corresponds to the relationship $|\underline{\Gamma}_{in}| = 1$. The complementary set of these regions corresponds to the region of instability with $|\underline{\Gamma}_{in}| > 1$.

Similarly, the stability region of the source (generator) is defined, thus:

$$\left|\underline{\Gamma}_G - \underline{c}_G\right| > r_G, \text{ daca } D_1 > 0; \; \left|\underline{\Gamma}_G - \underline{c}_G\right| < r_G, \text{ daca } D_1 < 0. \tag{4.6}$$

In order to have unconditional stability, the stability regions must contain the entire unit circle. If $D_2 > 0$, the unit circle and the load stability circle must not overlap at all, as

shown in Figure 4.1. Geometrically, the distance between points A and O from figure 4.1 is $(OA) = |\underline{c}_L| - r_L$. The disjunction of the circles requires that the condition to be satisfied is $(OA) > 1$ or equivalently $|\underline{c}_L| - r_L > 1$, [34 - 37].
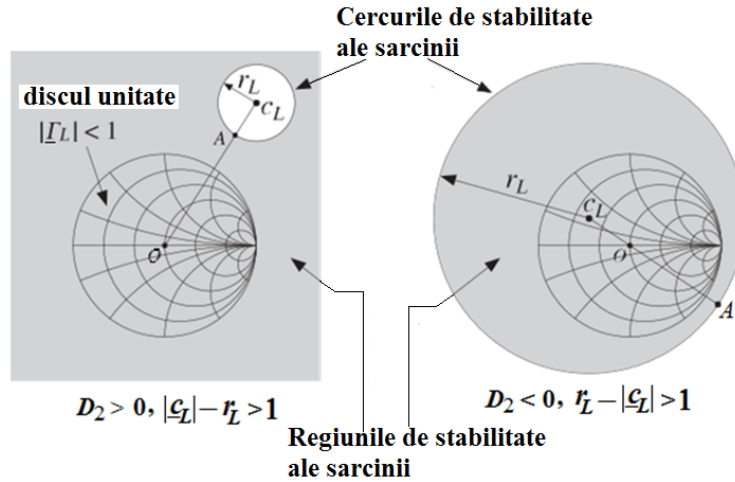

Fig. 4.1. Stability regions in the case of unconditional stability.

The stability conditions (4.5) can be combined into a single one and it is $sign(D_2)*|\underline{c}_L| - r_L > 1$, which is equivalent with $\mu_1 > 1$. Geometrically, the parameter μ_1 represents the distance (OA). So, the condition for the unconditional stability of the entrance is equivalent to:

$$\mu_1 > 1 \text{ - unconditional stability condition} \tag{4.7}$$

Edwards and Sinsky showed that only the condition (4.7) (or, alternatively, only the condition $\mu_2 > 1$) is necessary and sufficient for the unconditional stability of both the input and output impedances for a two-port circuit. Obviously, the stability regions of the source are similar to those in figure 4.1.

Any of the following criteria shall be necessary and sufficient for unconditional stability, [36, 38]:

$$K > 1 \text{ and } \left|\underline{\Delta}\right| < 1; K > 1 \text{ and } B_1 > 0; K > 1 \text{ and } B_2 > 0;$$

$$K > 1 \text{ and } \left|\underline{S}_{12}\underline{S}_{21}\right| < 1 - \left|\underline{S}_{11}\right|^2; K > 1 \text{ and } \left|\underline{S}_{12}\underline{S}_{21}\right| < 1 - \left|\underline{S}_{22}\right|^2. \tag{4.8}$$

All criteria (4.8) are equivalent to $\mu_1 > 1$.

Figure 4.2 illustrates a case of potential instability. If $D_2 > 0$, then $\mu_1 < 1$ is equivalent with $|\underline{c}_L| - r_L < 1$ and if $D_2 < 0$, is equivalent with $r_L - |\underline{c}_L| < 1$. In any case, the unit circle is partially superimposed on the stability circle, as shown in figure 4.2. The portion of the unit circle that is not located (stretched) inside the stability region corresponds to an impedance $\underline{Z}_{in}$ unstable.
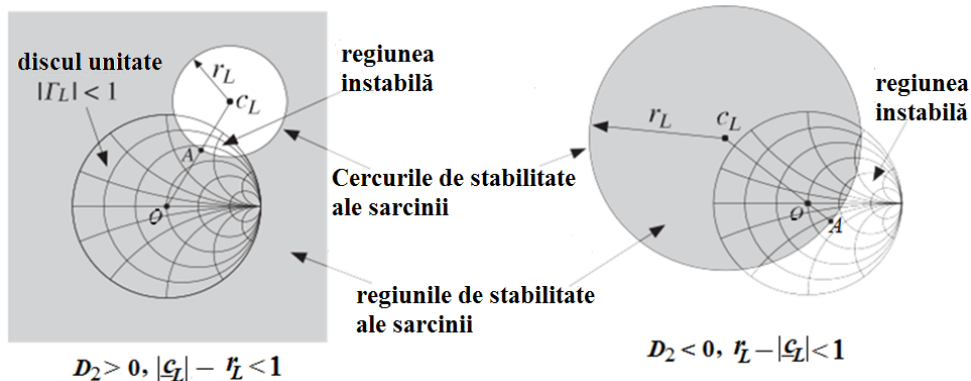

Fig. 4.2. Stability regions in case of potential instability.

Five widely used definitions for the power gain of a two-port circuit are: *the captured power gain G_t, the available power gain G_a* and *the gain (efficiency) of power transfer G_p, also called the operating gain, the maximum available gain G_{MAG}* and *the maximum stable gain G_{MSG},* [36, 38] (fig. 4.3).

Three definitions widely used for the power gain of the two-port circuit are: the captured power gain (of the transducer) G_t, the available power gain G_a and the power gain G_p, also called the operating gain, [30, 38] (fig. 4.3).
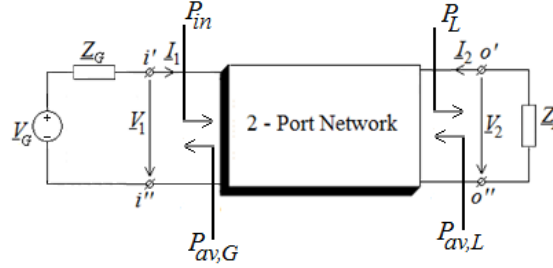

Fig. 4.3. Definition of power gains.

These gains can be expressed according to the parameters $\underline{S}$, $\underline{Z}$ and the coefficients of reflection, thus:

$$
G_T = \frac{P_L}{P_{av,G}} = \frac{1-\left|\underline{\Gamma}_G\right|^2}{\left|1-\underline{\Gamma}_{in}\underline{\Gamma}_G\right|^2}\left|\underline{S}_{21}\right|^2\frac{1-\left|\underline{\Gamma}_L\right|^2}{\left|1-\underline{S}_{22}\underline{\Gamma}_L\right|^2} =
$$
$$
= \frac{1-\left|\underline{\Gamma}_L\right|^2}{\left|1-\underline{\Gamma}_{out}\underline{\Gamma}_L\right|^2}\left|\underline{S}_{21}\right|^2\frac{1-\left|\underline{\Gamma}_G\right|^2}{\left|1-\underline{S}_{11}\underline{\Gamma}_G\right|^2}
$$
, (4.16)

$$
G_a = \frac{P_{av,L}}{P_{av,G}} = \frac{R_G}{R_{out}}\left|\frac{\underline{Z}_{21}}{\underline{Z}_{11}+\underline{Z}_G}\right|^2 = \frac{1-\left|\underline{\Gamma}_G\right|^2}{\left|1-\underline{S}_{11}\underline{\Gamma}_G\right|^2}\left|\underline{S}_{21}\right|^2\frac{1}{1-\left|\underline{\Gamma}_{out}\right|^2},
$$
(4.17)

and

$$
G_p = \eta_{21} = \frac{P_L}{P_{in}} = \frac{R_L}{R_{in}}\left|\frac{\underline{Z}_{21}}{\underline{Z}_{11}+\underline{Z}_G}\right|^2 = \frac{1}{1-\left|\underline{\Gamma}_{in}\right|^2}\left|\underline{S}_{21}\right|^2\frac{1-\left|\underline{\Gamma}_L\right|^2}{\left|1-\underline{S}_{22}\underline{\Gamma}_L\right|^2}.
$$
(4.18)

The captured power gain is maximized when the two-port circuit is simultaneously adapted, and that is when $\underline{\Gamma}_{in} = \underline{\Gamma}_G^*$ și $\underline{\Gamma}_L = \underline{\Gamma}_{out}^*$. The maximum power gain reached, when the two-port circuit is simultaneously adjusted, is called the maximum available power gain:

$$
G_{T,max} = G_{a,max} = G_{p,max} = G_{MAG}.
$$
(4.19)

The necessary and sufficient condition for simultaneous adaptation is $K \geq 1$, where K is the Rollet stability factor. G_{MAG} can be shown to have the expression:

$$
G_{MAG} = \frac{|S_{21}|}{|S_{12}|}\left(K - \sqrt{K^2 - 1}\right),
$$
(4.20)

called *the maximum available power gain.*

Maximum stability gain (G_{MSG}) represents the maximum value of G_{MAG}, which is obtained when $K = 1$:

$$
G_{MSG} = \frac{|S_{21}|}{|S_{12}|},
$$
(4.21)

called *maximum stability gain.*

Stationary wave ratio (SWR) σ is defined by the relationship:

$$
\sigma = SWR = \frac{V_{max}}{V_{min}} = \frac{1+\left|\underline{\Gamma}\right|}{1-\left|\underline{\Gamma}\right|}.
$$
(4.22)

In order to facilitate the study of the stability of the system consisting of two magnetically coupled coils, considered as passive linear two-port circuit in the harmonic regime, using S parameters, functions were developed in MATLAB.

4.3. Example

The printed coils represented in Figure 4.4, a are considered and the spice equivalent scheme, obtained with the ANSYS EXTRACTOR Q3D program [17], of the two magnetically coupled coils is given in Figure 4.4, b.

First, with the SYSEG program, [15], the expressions of S parameters were generated according to the frequency. By running the functions and routines implemented in MATLAB and in MAPLE, for the example considered, the results that will be exposed below were obtained.

Figure 4.5 shows that the modules of parameters S_{11} and S_{22} (S_{12} and S_{21}) show minimums (maximums and minimums) at the same frequencies, although the values of these extremes are not identical.

Figure 4.6 shows the variations with the frequency of active power transfer efficiencies η_{21} (from input to output) and η_{12} (from output to input), $Gp*100$ and of signal transmission efficiencies η_{21_S21} – from input to output and η_{12_S12} – from output to input. From Figure 4.6 it is observed that the efficiencies η_{21} and $Gp*100$ have identical variations with the frequency and the maximum value of the efficiency is 88.7 % at a frequency of 13.89 MHz.
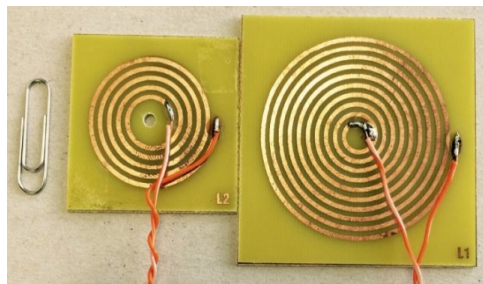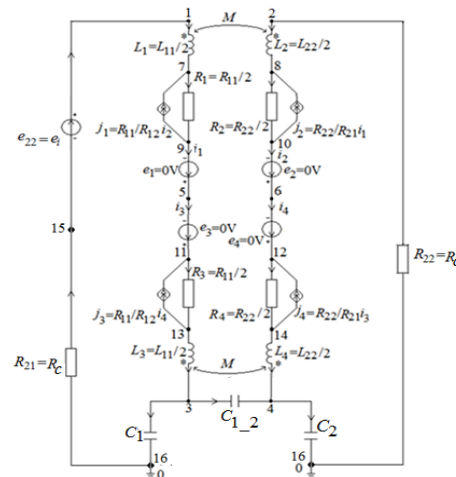
(a)   (b)

Fig. 4.4 a) The structure of the two printed coils (pcb spiral Coils); b) Spice equivalent circuit obtained with the Q3D EXTRACTOR program.
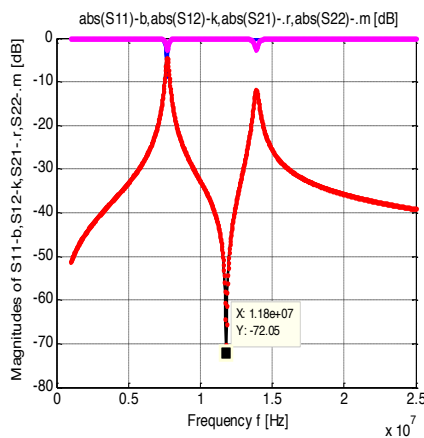

Fig. 4.5. mag(S_{11}), mag(S_{12}), mag(S_{21}) și mag(S_{22}) depending on the frequency.

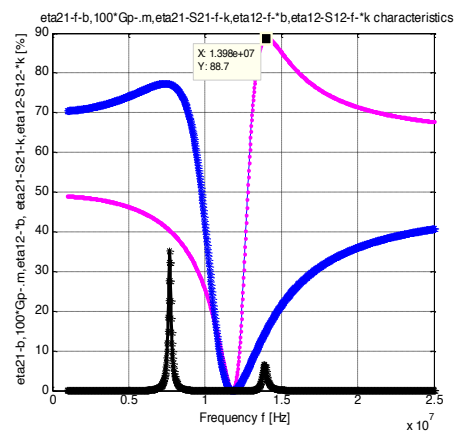**Fig. 4.6.** Efficiencies eta21-b, 100*Gp-.m, eta12-*b, eta21-S21-k, eta12-S12-*k depending on the frequency.

Figure 4.7 represents the variations with the frequency of the gains: of captured power G_t, of available power G_a, of operation (efficiency) G_p, of maximum power G_{mag} and of maximum stable power G_{msg}.

Figure 4.8 shows the variations with the frequency of the stationary wave ratio in relation to: the coefficient of reflection of: source, load, in relation to the input and in relation to the output.
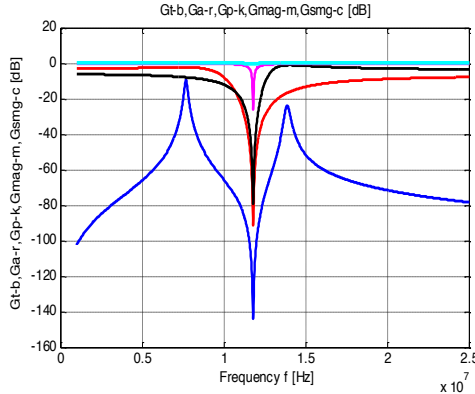

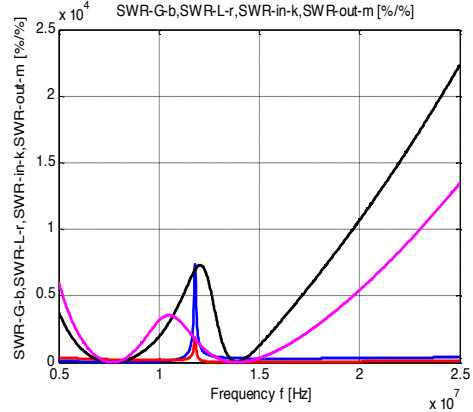**Fig. 4.7.** Variations with the frequency of gains G_t, G_a, G_p, G_{mag} and G_{msg}.

Fig. 4.8. SWR-$\underline{\Gamma}_G$-b, SWR-$\underline{\Gamma}_L$ -r, SWR-$\underline{\Gamma}_{in}$ -k and SWR-$\underline{\Gamma}_{out}$ -m depending on the frequency.

In Figure 4.9 (fig. 4.10) are shown the variations with frequency of the stability coefficient $k_{stab} = |\underline{\Gamma}_G - \underline{c}_G| - r_G$ and constant D_1 ($k_{stab} = |\underline{\Gamma}_L - \underline{c}_L| - r_L$ and constant D_2). It is found that the system of two magnetically coupled coils analyzed is stable throughout the frequency variation range, because there are satisfied inequalities $|\underline{\Gamma}_G - \underline{c}_G| > r_G$, if $D_1 > 0$; $|\underline{\Gamma}_G - \underline{c}_G| < r_G$, if $D_1 < 0$ ($|\underline{\Gamma}_L - \underline{c}_L| > r_L$, if $D_2 > 0$; ($|\underline{\Gamma}_L - \underline{c}_L| < r_L$, if $D_2 < 0$).
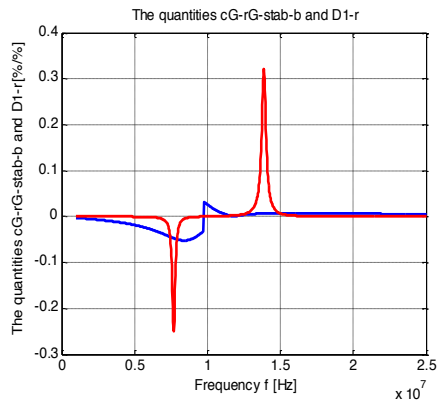

Fig. 4.9. Variations with the frequency of the stability coefficient $k_{stab} = |\underline{\Gamma}_G - \underline{c}_G| - r_G$ and constant D_1.
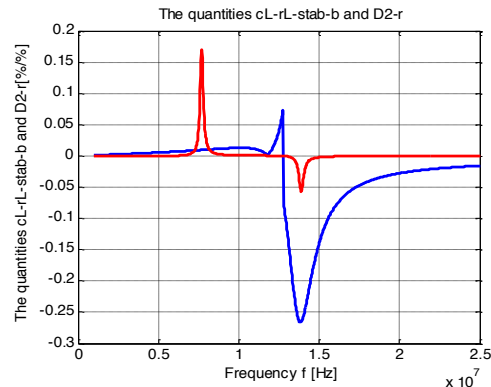
Fig. 4.10. Variations with the frequency of the stability coefficient $k_{stab} = |\underline{\Gamma}_L - \underline{c}_L| - r_L$ and constant D_2.
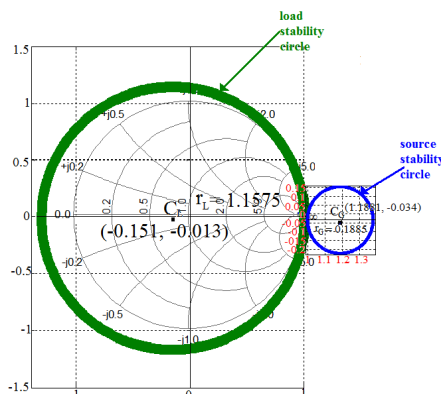

Fig.4.11. The stability circles of the source and load at the frequency of 13.768 MHz.

31

Figure 4.11 shows, on the Smith diagram, the stability circles of the source and load.

4.4. Conclusions

Starting from the correct definition of the $\underline{S}$ parameters (based on the circuit theory) the matrix $\underline{\pmb{S}}$ of the scattering parameters is automatically generated, and then, based on this matrix, the $\underline{\pmb{Z}}$, $\underline{\pmb{Y}}$ and $\underline{\pmb{T}}$ matrices are calculated. Considering the two magnetically coupled coils (resonators) used in the wireless transfer of power as a passive linear two-port circuit in the harmonic mode, it is determined: complex input and output impedances, $\underline{Z}_{in}$ și $\underline{Z}_{out}$; coefficients of reflection: $\underline{\Gamma}_{G}$, $\underline{\Gamma}_{L}$, $\underline{\Gamma}_{in}$ și $\underline{\Gamma}_{out}$; transfer functions e_c (u_C); stability coefficients: K – Rollet stability factor, μ_1 and μ_2 – stability factors, the centers and radii of the source and load stability circles, various constants necessary to define the stability factors and there are deduced the relationships between these quantities and the $\underline{S}$ parameters. There is exposed the practical way of using these parameters in streamlining the processes of transmission and propagation of information and the wireless transfer of electromagnetic energy from the point of view of transmission of signals from the transmitter to the receiver and from the point of view of the efficiency of the transfer of the active power from the input of the wireless systems to the loads connected to their output. Based on the theorem of the maximum active power transfer theorem, the maximum active power transmitted by a SWTP to the load is calculated and, depending on S parameters, the most widely used performance coefficients are determined in practice: the captured power gain G_t, the available power gain G_a, the gain (efficiency) of power transfer G_p, also called the operating gain, the maximum power gain and the stable maximum power gain. The necessary and sufficient conditions have been established for two magnetically coupled coils (equivalated to a passive linear two-port circuit) to be *unconditionally stable.* In the paper was elaborated a procedure of generating, on the Smith diagram, the stability circles corresponding to the source and the load.

At the end, procedures have been developed and implemented for the calculation of: reflection coefficients, stationary wave ratios (SWR), input and output impedances, efficiencies of active power transmission from input to output (output to input), signal transmission efficiencies, power gains, various stability coefficients, the centers and radii of the stability circles at the source and the generator, the $\underline{\pmb{S,}}$ $\underline{\pmb{T}}$, $\underline{\pmb{Z}}$ and $\underline{\pmb{Y}}$ matrices and Smith diagrams. The results obtained by simulations were compared with those presented in the literature and with the experimental ones.

The accuracy of the calculations and of the graphic representations, obtained by simulations, is confirmed by the results obtained with the ADS program, endowed with specific subroutines for the generation of $\underline{S}$ parameters and other quantities necessary to determine the stability regions of the wireless power transfer systems.

5. CALCULATION OF THE *KQ* FIGURE OF MERIT AND THE PROPERTIES OF WIRELESS ELECTROMAGNETIC POWER TRANSFER SYSTEMS

5.1. Introduction

Most engineers in the 20th century believed that the inductive transfer of power was due to the coupling coefficient *k* between the two coils. Kurs and his collaborators in 2007 [23] demonstrated that although the coupling factor *k* is small, a powerful wireless power transfer can be performed if the quality factor *Q* of the two magnetically coupled coils is improved. Therefore, the *kQ* product being a real number, it can meet the requirements to work as a *figure of merit (FoM)*, [5, 39 – 41, 42, 43].

In this chapter it will be demonstrated how the *kQ* product can be calculated according to the conventional parameters $\underline{Z}$, $\underline{Y}$, $\underline{T}$ or $\underline{S}$ of the electrical two-port circuit systems.

The magnetically coupled coil system, used in the wireless transfer of electromagnetic power, can be described as a passive linear two-port circuit (fig. 5.1).
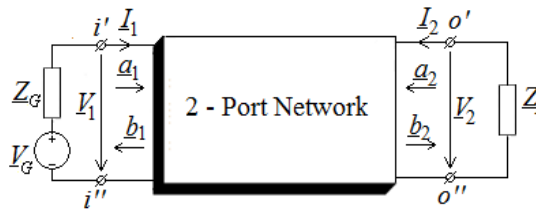

Fig. 5.1. Passive linear two-port circuit connected to the generator and load.

To be able to compare between them, unambiguously, different wireless power transfer systems, *FoM* must be a unique scalar number. It is preferable for *FoM* to be a dimensionless size. These requirements are significant problems for two-port electrical systems, since they are characterized, in the harmonic regime at low frequencies, by complex matrices $\underline{Z}$, $\underline{Y}$ and $\underline{T}$ that have the size of *immittances* [41, 43]. At high frequencies, the $\underline{Z}$, $\underline{Y}$ and $\underline{T}$ matrices can be expressed according to the $\underline{S}$ parameters, which can be measured with the network vector analyzer (VNA). To calculate *FoM* that meets the above requirements, the first step is to break down complex numbers into their real and imaginary parts.

This chapter presents three definitions for the *kQ* figure of merit. All three definitions are based on the electrical circuit theory. The calculation of the *kQ* figure of merit for various configurations of two-port circuit systems is carried out simply, using a circuit simulator. Three significant examples are given that validate the correctness of the definition and calculation methods set out.

5.2. Calculation of the *kQ* figure of merit

The simplest expression of the *kQ* figure of merit, for a two-port circuit system consisting of two magnetically coupled coils, is given by the relation, [8, 13, 14]:

$$kQ\_1 = k \cdot \sqrt{Q_1 \cdot Q_2},$$

$$(5.1)$$

where: k is the coupling coefficient of the two coils, $k = M / \sqrt{L_1 \cdot L_2}$, and $Q_1 = \omega L_1 / R_1$, $Q_2 = \omega L_2 / R_2$ are the quality factors of the transmitting coil and of the receiving coil.

For complex structures of bipolar systems (circuits) the figure of merit is defined according to the real and imaginary parts of the matrix of complex impedances $\underline{Z}$. The matrix of the complex impedances of a two-port circuit system, which operates in harmonic regime, has the structure:

$$\underline{Z} = \begin{bmatrix} \underline{Z}_{11} & \underline{Z}_{12} \\ \underline{Z}_{21} & \underline{Z}_{22} \end{bmatrix} = \begin{bmatrix} R_{11} & R_{12} \\ R_{21} & R_{22} \end{bmatrix} + j \begin{bmatrix} X_{11} & X_{12} \\ X_{21} & X_{22} \end{bmatrix} = \boldsymbol{R} + j\boldsymbol{X}. \tag{5.2}$$

The module of the impedance $\underline{Z}_{21}$, $\left| \underline{Z}_{21} \right| = \sqrt{R_{21}^2 + X_{21}^2}$, can be considered as a figure of merit. However, since *FoM* is a dimensionless size, we must find a quantity with the same size as the module of $\underline{Z}_{21}$, by which to divide this module. Therefore, it is considered as the denominator for the figure of merit, the square root of the determinant of the resistance matrix, called *Equivalent Scalar Resistance* (*ESR*).

$$ESR = \sqrt{R_{11}R_{22} - R_{12}R_{21}}. \tag{5.3}$$

Then, the figure of merit kQ_2 has the expression:

$$kQ_{\_2} = \frac{\left| \underline{Z}_{21} \right|}{\sqrt{R_{11}R_{22} - R_{12}R_{21}}}. \tag{5.4}$$

In the paper [6] it is proposed for the calculation of the figure of merit kQ, for a two-port circuit system of power transmission, the following formula:

$$kQ_{\_3} = \sqrt{\frac{R_{11}R_{22} + X_{12}X_{21}}{R_{11}R_{22} - R_{12}R_{21}}}. \tag{5.5}$$

With the above definitions of kQ, the maximum efficiency of a power transmission system can thus be expressed:

$$\eta_{max} = \frac{kQ - 1}{kQ + 1}. \tag{5.6}$$

The variation in the efficiency of power transmission as a function of the figure of merit is shown in figure 5.2.

The matrix of complex impedances $\underline{Z}$ can be expressed according to the matrix of the $\underline{S}$ parameters, by the relation, [6]:

$$\underline{Z} = \left(\boldsymbol{I}_2 - \underline{\boldsymbol{S}} \right)^{-1} \cdot \left(\boldsymbol{I}_2 + \underline{\boldsymbol{S}} \right) Z_0, \tag{5.7}$$

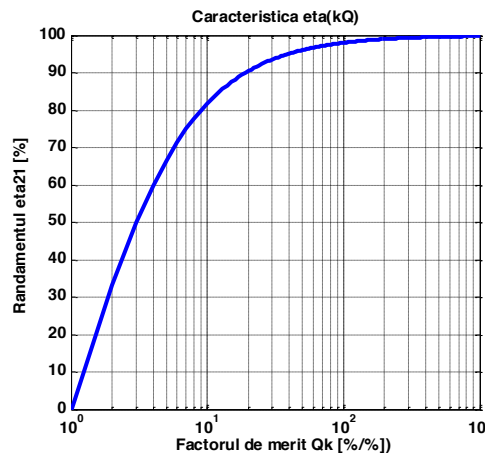where $\boldsymbol{I}_2$ is the unit matrix of order 2.

Fig. 5.2. Variation of the maximum efficiency η_{21_max} depending on the kQ figure of merit.

The input impedance (from the terminals $i' - i''$) $\underline{Z}_{in}$ is defined as follows:

$$\underline{Z}_{in} = \underline{Z}_{11} - \frac{\underline{Z}_{12}\underline{Z}_{21}}{\underline{Z}_L + \underline{Z}_{22}}, \tag{5.8}$$

The output impedance (from the terminals $o' - o''$) $\underline{Z}_{out}$ is defined by the relation:

$$\underline{Z}_{out} = \underline{Z}_{22} - \frac{\underline{Z}_{12}\underline{Z}_{21}}{\underline{Z}_G + \underline{Z}_{11}}. \tag{5.9}$$

The input and output impedances $\underline{Z}_{in}$ and $\underline{Z}_{out}$ allow the substitution, according to the theorem of the equivalent voltage generator (Thévenin's theorem), of the passive linear two-port circuit in figure 5.1 with the equivalent circuits represented in figure 5.3, [6, 14, 15, 44].
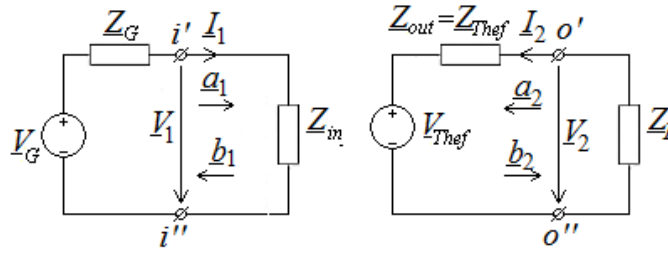

Fig. 5.3. Equivalent circuits at the input and output of a passive linear two-port circuit.

The voltage $\underline{V}_{Thef} = \underline{V}_2\big|_{I_2=0, V_1=V_G-Z_G I_1} = \frac{\underline{Z}_{21}}{\underline{Z}_G + \underline{Z}_{11}}\underline{V}_G$, and $\underline{Z}_{Thef} = \frac{\underline{V}_{Thef}}{\underline{I}_{2\_0}} = \underline{Z}_{out}$.

The efficiency of the transmission of the active power from the transmitting coil (from the input terminals $i' - i''$) to the load (at the output terminals $o' - o''$) can be calculated with the relation:

$$\eta_{21} = \frac{P_2}{P_1} \cdot 100 = \frac{R_L}{R_{in}} \cdot \left|\frac{\underline{Z}_{21}}{\underline{Z}_{22} + \underline{Z}_L}\right|^2 \cdot 100, \tag{5.10}$$

where $R_{in} = \mathrm{Re}(\underline{Z}_{in})$ and $R_L = \mathrm{Re}(\underline{Z}_L)$.

The efficiency of transmitting signals from the transmitting coil (from the input terminals $i' - i''$) to the load (at the output terminals $o' - o''$) has the expression:

$$\eta_{21\_S_{21}} = \underline{S}_{21} \cdot \underline{S}_{21}^* \cdot 100 = \left|\underline{S}_{21}\right|^2 \cdot 100, \tag{5.11}$$

And the signal transmission efficiency from the receiving coil (from the output terminals $o' - o''$) to the generator (at the input terminals $i' - i''$) is calculated with the relation:

$$\eta_{12\_S_{12}} = \underline{S}_{12} \cdot \underline{S}_{12}^* \cdot 100 = \left|\underline{S}_{12}\right|^2 \cdot 100. \tag{5.12}$$

According to the theorem of the maximum power transfer, the load receives maximum power if $\underline{Z}_L = \underline{Z}_{out}^*$ and it has the expression:

$$P_{L\_max} = \frac{V_{Thef}^2}{4 \cdot \mathrm{Re}\left(\underline{Z}_{out}\right)}. \tag{5.13}$$

5.3. Example

As an example, the linear two-port circuit from figure 5.4 is considered to be the equivalent circuit of a magnetically coupled resonator with a combined series-parallel topology, used in the wireless power transfer.
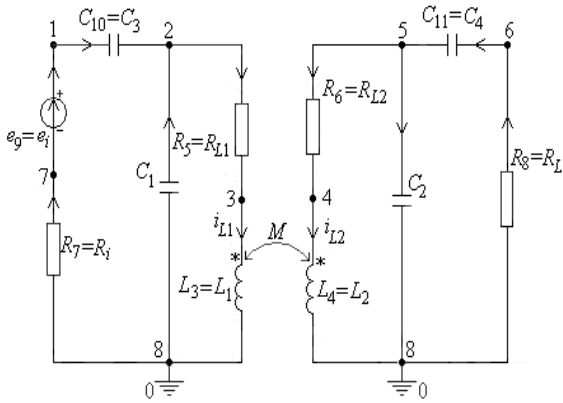
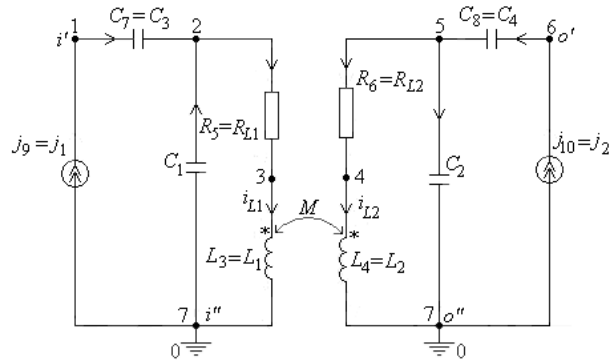**Fig. 5.4.** The equivalent circuit of a magnetically coupled resonator with a combined series-parallel topology.

Fig. 5.5. Connection of independent current sources j_1 and j_2 to the entry-output gates of the circuit in figure 5.4, for the calculation of the elements of the $\underline{Z}$ matrix.

Figure 5.6 (fig. 5.7) shows the frequency variations of the figure of merit (of the maximum power transmission efficiency) for the three expressions of the figure of merit.
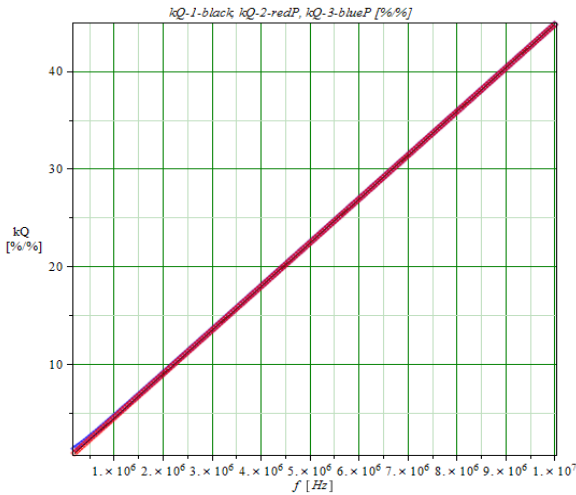

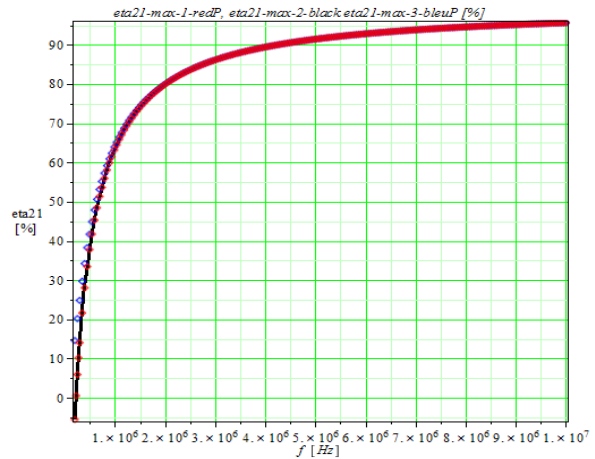**Fig. 5.6.** Variations with the frequency of the figure of merit for the three formulas.

Fig. 5.7. Variations with the frequency of the maximum efficiency for the three formulas for calculating the figure of merit.

From figures 5.6 and 5.7 it is found that the values of the figure of merit, respectively of the maximum efficiency, at different frequencies, are the same for the three formulas for calculating the figure of merit.

For the resonance frequency $f_0 = 1.805$ MHz of the resonator in figure 5.4, the three figures of merit and the corresponding three maximum efficiencies have the values in the Table 5.1.

Table 5.1. Figures of merit and the corresponding maximum efficiencies

$kQ_{\_1\_f0} = 8.07987$	$\eta_{max\_1\_f0} = 77.97326\%$
$kQ_{\_2\_f0} = 8.07987$	$\eta_{max\_2\_f0} = 77.97326\%$
$kQ_{\_3\_f0} = 8.14150$	$\eta_{max\_3\_f0} = 78.12180\%$

From Table 5.1 it is noticed that for the first two cases the values are identical, the values for the case 3 are higher, the errors being below 0.8%.

The circuit in figure 5.3 can also be analyzed using the ADS program. For this, in figure 5.8 was drawn the equivalent scheme of the circuit from figure 5.4 required by the ADS program.
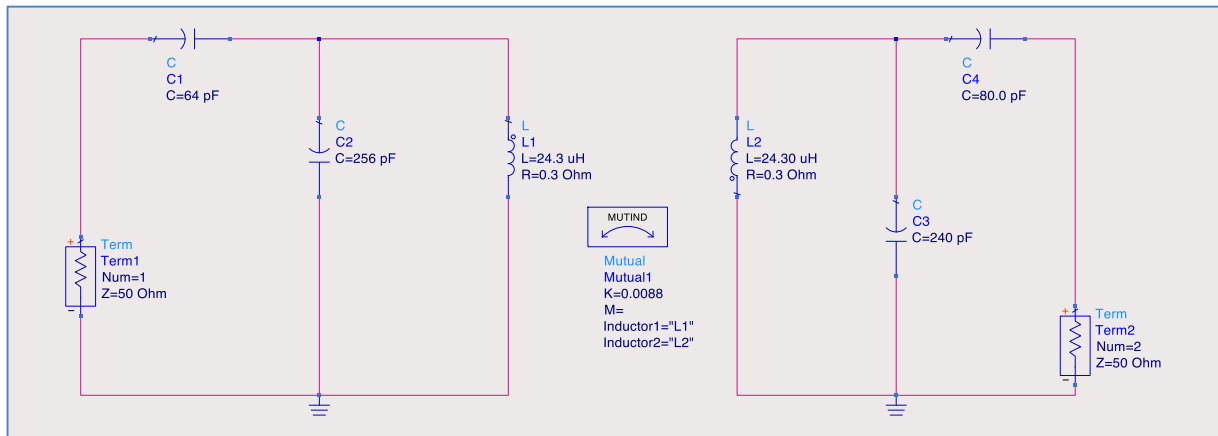
Fig. 5.8. Scheme of the circuit in figure 5.4, used by the ADS program.

The frequency variation of the active power transmission efficiency from the transmitter to the receiver $\eta_{21} = 100 * P_{2/P1}$ is shown in figure 5.9, and in figures 5.10 and 5.11 respectively the variations with the frequency of the magnitudes of the mag(S_{21}) and mag (S_{12}) parameters, respectively of the parameters mag(S_{11}) and mag (S_{22}) are exposed.

From figures 5.9 to 5.11 it is found that the extremes of the efficiency and magnitudes of the four S parameters correspond to the same values of the frequency $f_{rez} = 1.805$ MHz. Since the circuit in figure 5.8 is symmetrical, the variations with the frequency of the modules of the parameters S_{12} and S_{21} – figure 5.10 (S_{11} and S_{22} – figure 5.11) are identical.
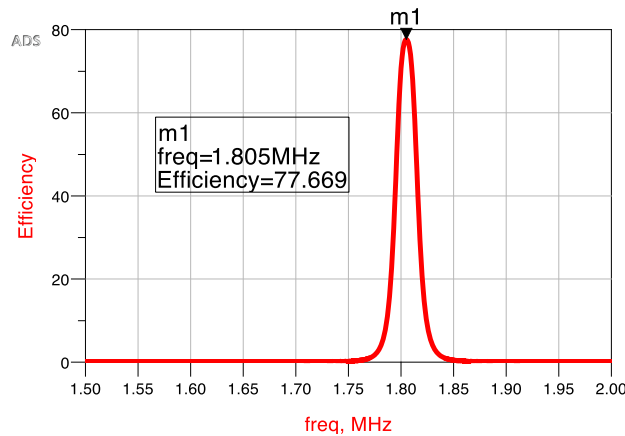

Fig. 5.9. Variation with the frequency of the efficiency η_{21}.
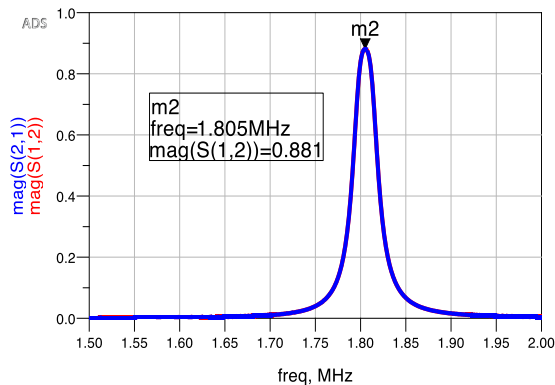
Fig. 5.10. Variations with the frequency of parameter magnitudes: mag(S_{21}) and mag (S_{12}).
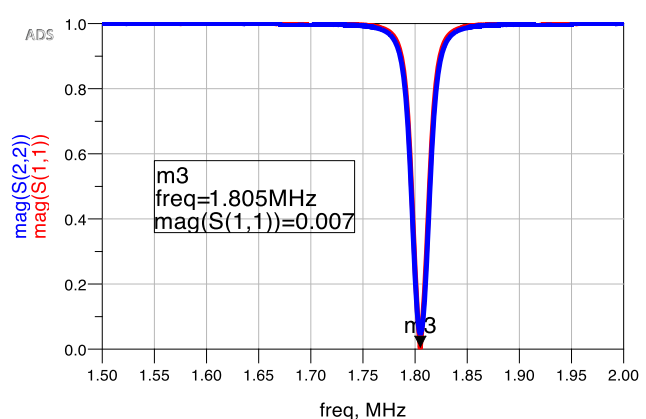
Fig. 5.11. Variations with the frequency of parameter magnitudes: mag(S_{11}) and mag (S_{22}).
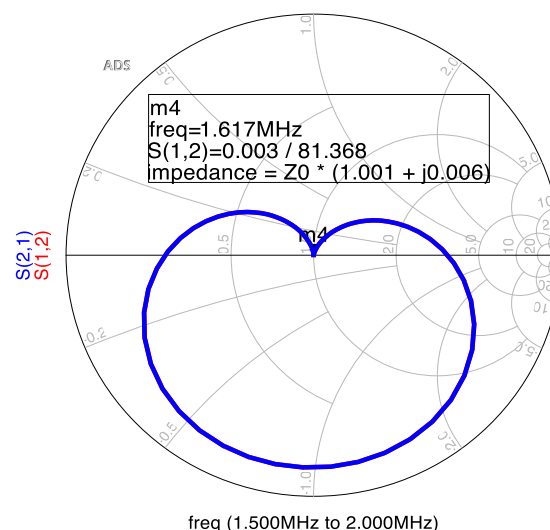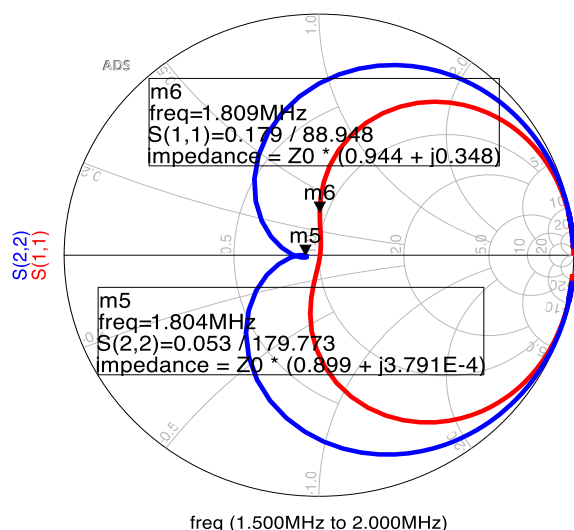
Fig. 5.12. Representation of parameters $\underline{S}_{11}$ and $\underline{S}_{22}$ on the Smith diagram.

Fig. 5.13. Representation of parameters $\underline{S}_{12}$ și $\underline{S}_{21}$ on the Smith diagram.

The figure 5.12 (fig. 5.13) shows the mode of variation with the frequency on the Smith diagram, [6], of the parameters $\underline{S}_{11}$ și $\underline{S}_{22}$ ($\underline{S}_{12}$ and $\underline{S}_{21}$).

5.4.   Conclusions

In this chapter was introduced the *quality factor* (the *figure of merit*) of the transmission, which is more general and accurate than the figure of merit used in the literature. Based on a generalized transmission system, an explicit definition has been developed for *the kQ* product - called Figure of Merit – *FoM*, as a new property of power transmission systems, which allows to easily determine the charging range in the system and allows it to operate efficiently.

It is proved that the merit factor of a power transfer system can be calculated according to its conventional parameters $\underline{Z}$, $\underline{Y}$, $\underline{T}$ or $\underline{S}$. The **$\underline{Z}$, $\underline{Y}$, $\underline{T}$** and **$\underline{S}$** matrices can be calculated using an electrical circuit simulator, if an equivalent system scheme is available. Otherwise, for a real system these matrices can be measured using a vector network analyzer (VNA).

The presented examples fully confirm the correctness of the definitions given to the figure of merit and demonstrates the usefulness of the transfer factor in the analysis of the efficiency of the power transfer in the electrical two-port circuit systems. Also, the examples presented confirm that the merit factor *kQ* has the following properties: 1) is a *dimensionless real number*; 2) it can be inferred from the parameters of immittances; 3) represents the transfer characteristics of the two-port circuits; 4) is invariably in relation to the conditions of source and load and 5) functions as an *essential FoM* for passive systems.

6. CONCLUSIONS

6.1. General conclusions

To characterize linear devices, in harmonic mode, at low and medium frequencies, these parameters are used: $\underline{Z}$, $\underline{Y}$, $\underline{H}$, $\underline{T}$ etc. When these devices operate at high and very high frequencies these parameters cannot be used, since they require circuits with certain short circuits or left in the void (interrupted) for taking measurements so that the currents and voltages in the circuit can be calculated.

At high and very high frequencies, for the qualitative analysis of analog circuits, you can use the scattering (distribution) parameters – noted $\underline{S}$, which are complex sizes, depending on frequency, associated with a linear multiport system, in the harmonic regime.

The correct definition, based on the theory of electrical circuits, of $\underline{S}$ parameters allowed their automatic generation, using the state equations or the modified nodal equations.

Programs used to generate $\underline{S}$ parameters for various magnetically coupled resonator configurations, CADENCE; ADS; ANSOFT EXTRACTOR, FEKO, SYSEG și SCAP, have validated the correctness of the formulas (2.6) – (2.9) for the definition of $\underline{S}$ parameters.

Considering the two magnetically coupled coils (resonators) used in wireless power transfer as a passive linear two-port circuit in the harmonic mode, the $\underline{S}$ parameters for all types of connections are determined. The paper shows the practical way of using these parameters in streamlining the processes of transmission and propagation of information and of the wireless transfer of electromagnetic energy from the transmitter to the receiver.

Once the $\underline{S}$ parameters have been generated, for a set of frequencies, there can be generated: $\underline{\boldsymbol{T}}$, $\underline{\boldsymbol{Z}}$ and $\underline{\boldsymbol{Y}}$ matrices; $\underline{\Gamma}_G$, $\underline{\Gamma}_L$, $\underline{\Gamma}_{in}$ and $\underline{\Gamma}_{out}$ reflection coefficients; active power transmission efficiencies η_{21} and η_{12}; signal transmission efficiencies η_{21_S21} and η_{12_S12}; input and output impedances $\underline{Z}_{in}$ and $\underline{Z}_{out}$; Thévenin equivalent generator; the captured power gain G_t, available power gain G_a and the gain (efficiency) of power transfer G_p, also called the operating gain and Smith diagrams for $\underline{S}$ parameters.

For the analysis of the stability of wireless electrical power transfer systems, the matrix $\underline{\boldsymbol{S}}$ of the scattering parameters is automatically generated, and then, based on this matrix, the $\underline{\boldsymbol{Z}}$, $\underline{\boldsymbol{Y}}$ and $\underline{\boldsymbol{T}}$ matrices are calculated. Considering the two magnetically coupled coils (resonators) used in the wireless transfer of power as a passive linear two-port circuit in the harmonic mode, it is determined: complex input and output impedances, $\underline{Z}_{in}$ și $\underline{Z}_{out}$; coefficients of reflection: $\underline{\Gamma}_G$, $\underline{\Gamma}_L$, $\underline{\Gamma}_{in}$ și $\underline{\Gamma}_{out}$; transfer functions e_c (u_C); stability coefficients: K – Rollet stability factor, μ_1 and μ_2 – stability factors, the centers and radii of the source and load stability circles, various constants necessary to define the stability factors and there are deduced the relationships between these quantities and the $\underline{S}$ parameters. There is exposed the practical way of using these parameters in streamlining the processes of transmission and propagation of information and the wireless transfer of electromagnetic energy from the point of view of transmission of signals from the transmitter to the receiver and from the point of view of the efficiency of the transfer of the active power from the input of the wireless systems to the loads connected to their output. Based on the theorem of the maximum active power transfer theorem, the maximum active power transmitted by a SWTP to the load is calculated and, depending on $\underline{S}$ parameters, the most widely used performance coefficients are

determined in practice: the captured power gain G_t, the available power gain G_a, the gain (efficiency) of power transfer G_p, also called the operating gain, the maximum power gain and the stable maximum power gain. The necessary and sufficient conditions have been established for two magnetically coupled coils (equivalated to a passive linear two-port circuit) to be *unconditionally stable.* In the paper was elaborated a procedure of generating, on the Smith diagram, the stability circles corresponding to the source and the load.

At the end, procedures have been developed and implemented for the calculation of: reflection coefficients, stationary wave ratios (SWR), input and output impedances, efficiencies of active power transmission from input to output (output to input), signal transmission efficiencies, power gains, various stability coefficients, the centers and radii of the stability circles at the source and the generator, the ***S, T*, *Z*** and ***Y*** matrices and Smith diagrams. The results obtained by simulations were compared with those presented in the literature and with the experimental ones.

The accuracy of the calculations and of the graphic representations, obtained by simulations, is confirmed by the results obtained with the ADS program, endowed with specific subroutines for the generation of *S* parameters and other quantities necessary to determine the stability regions of the wireless power transfer systems.

In Chapter 5 was introduced the *quality factor* (the *figure of merit*) of the transmission, which is more general and accurate than the figure of merit used in the literature. Based on a generalized transmission system, an explicit definition has been developed for *the kQ* product - called Figure of Merit – *FoM*, as a new property of power transmission systems, which allows to easily determine the charging range in the system and allows it to operate efficiently.

It is proved that the merit factor of a power transfer system can be calculated according to its conventional parameters *Z, Y, T* or *S*.

The presented examples fully confirm the correctness of the definitions given to the figure of merit and demonstrates the usefulness of the transfer factor in the analysis of the efficiency of the power transfer in the electrical two-port circuit systems. Also, the examples presented confirm that the merit factor *kQ* has the following properties: 1) is a *dimensionless real number*; 2) it can be inferred from the parameters of immittances; 3) represents the transfer characteristics of the two-port circuits; 4) is invariably in relation to the conditions of source and load and 5) functions as an *essential FoM* for passive systems.

6.2. Original contributions

The main original contributions made by the author in the thesis are:
- ✓ An in-depth documentation on the topic was made, the results being synthesized in a useful manner to further research in the field.
- ✓ Correct definition of *S* parameters, using the theory of electrical circuits, and several effective procedures for calculating these parameters have been exposed.
- ✓ Elaboration of efficient routines in the MAPLE and MATLAB programming environments, suitable for all procedures for simulation of analog multiport circuits.
- ✓ Automatic calculation of the parameters associated with a linear quadrupole in the harmonic regime.
- ✓ Elaboration of an efficient algorithm for the complete analysis of analog filters and the implementation of this algorithm in a high-performance program.
- ✓ Adaptation of the SCAP program for the symbolic, partially symbolic, and numerical formulation of the modified nodal equations in operational.
- ✓ Adaptation of the SYSEG program for the symbolic, partially symbolic, and numerical formulation of the status equations in operational.
- ✓ The algorithm for calculating the S-parameters was elaborated in detail and this algorithm was implemented in a program in the MAPLE 18 environment, for the configuration of the resonator with series-series connection.

✓ Using the algorithm and program described above, the S parameters were calculated for the other three connections of the magnetically coupled resonators: series-parallel, parallel-series and parallel-parallel.

✓ The validation of the results obtained with the SCAP and SYSEG programs was carried out by comparing them with those calculated with the ADS and SPICE programs.

✓ Using the theory of electrical circuits, it was presented, starting from the matrix of parameters ___S___, the way of determining the main elements necessary for the qualitative analysis of the electrical circuits in harmonic regime: the matrix of complex impedances ___Z___, the matrix of complex admittances ___Y___, the matrix of complex transfer coefficients (fundamental) ___T___, complex input and output impedances, Z_{in} and Z_{out}, the coefficients of reflection from the generator Γ_G, from load Γ_L, from the input Γ_{in} and from the output Γ_{out}, the equivalent voltage generator (Thévenin equivalent circuit) in relation to the two-port output.

✓ Also, it was exposed the practical way of using S parameters in the efficiency of the processes of transmission and propagation of information and of the transfer of electromagnetic energy.

✓ Based on the theorem of the maximum active power transfer there was presented the way of calculating the maximum active power transmitted by a two-port circuit to the load.

✓ Development of an efficient Smith diagram generation algorithm and its use in the analysis of the performance of analog two-port and multiport circuits.

✓ Established the necessary and sufficient conditions for two magnetically coupled coils (equivalated to a passive linear two-port circuit) to be *unconditionally stable*.

✓ Procedures have been developed for the representation on the Smith diagram of the S parameters, the coefficients of reflection from: the generator, load, input and output, the impedances from the input and output, the admittances from the input and output, the transfer functions, etc.

✓ An explicit definition has been developed for *the kQ* product - called a Figure of Merit – *FoM*, which allows to easily determine the load range in the system and allows it to function efficiently.

✓ Elaboration, for each calculation procedure proposed in the thesis, of an efficient automatic calculation routine in the MAPLE and MATLAB programming environments.

✓ The results obtained through simulations were compared with those obtained experimentally on the wireless power transfer systems existing in the laboratories of Electrical Engineering Department within UPB. Errors were negligible.

It is specified that the results obtained in the research activity within the doctoral thesis were made known to the scientific community in the country and abroad in the form of scientific communications, participation in international conferences, articles in specialized journals. These papers were specified in the bibliography and were quoted in the thesis.

6.3. Perspectives of further development

Contributions on the use of S parameters and Smith's diagram in the analysis of analog circuits contained in this paper could be used in this way:

- Development of software applications for the analysis and modeling of analog circuits at high and very high frequencies using the presented models and algorithms.
- Deepening the research on the use of S parameters and smith diagram in the analysis of analog circuits at high and very high frequencies for cutting-edge areas such as aeronautics, military, medical, automotive, development of smart models for urban infrastructures, etc.
- A continuation of the research on the use of S parameters and the Smith Diagram in the analysis of analog circuits by future PhD students and PhDs in electrical engineering.

7. BIBLIOGRAPHY

[1]   *S. J. Orfanidis*, "Electromagnetic Waves and Antennas", 2008, link: http://www.ece.rutgers.edu/ orfanidi/ewa/.

[2]   *George Lojewski*, "Dispozitive şi circuite de microunde", Editura Tehnică, 2005

[3]   *Anca Tomescu, F. M. G. Tomescu*, "Microwave Systems", Editura MatrixROM, Bucursti, 2001.

[4]   *R. B. Marks and D. F. Williams*, "A general waveguide circuit theory", Journal of Research of the National Institute of Standards and Technology, No. 97, 1992, pp. 533–564.

[5]   *D. A. Frickey*, "Conversions between S, Z, Y, H, ABCD, and T parameters which are valid for complex source and load impedances," IEEE Trans. on Microwave Theory and Techniques, No. 42, 1994, pp. 205–211.

[6]   *R. B. Marks and D. F. Williams*, "Comments on conversions between S, Z, Y, H, ABCD, and T parameters which are valid for complex source and load impedances", IEEE Trans. on Microwave Theory and Techniques, No. 43, 1995, pp. 914–915.

[7]   *D. Ioan and Gabriela Ciuprina*, "Reduced Order Models of On-chip Passive Components and Interconnects, Workbench and Test Structures", Book chapter in the book "Model Order Reduction: Theory, Research Aspects and Applications", (W.H.A. Schilders, H.A. van der Vorst, J. Rommes, Eds.), in the book series Mathematics in Industry, Springer-Verlag, Heidelberg, No. 13, 2008, pp. 447-467.

[8]   *T. Imura, H. Okabe, Y. Hori*, "Basic Experimental Study on Helical Antennas of Wireless Power Transfer for Electric Vehicles by using Magnetic Resonant Couplings", Proceedings of Vehicle Power and Propulsion Conference, September 2009, IEEE Xplore, 978-1-4244-2601-4/010/2010, pp. 936-940.

[9]   *Gabriela Ciuprina, Aurel-Sorin Lup, Alina Tomescu*, "Parametrii *S* in aplicatii de inalta frecventa", SNET'12 Conference Proceedings, pag 216-221, 2012, disponibila la http://snet.elth.pub.ro/snet2012/volume/SNET2012Proceedings.pdf.

[10]   *Marilena Stănculescu, M. Iordache, D. Niculae, Lavinia Iordache, V. Bucată*, "*S* Parameter Computation and Their Use for Electromagnetic Energy Wireless Transmission", IJCT – International Journal of Computers & Technologies, Vol. 12, No, June 2016, pp. 37097-7108.

[11]   *A. Elsherbeni, P. Nayeri and C. J. Reddy*, "Antenna Analysis and Design Using FEKO Electromagnetic Simulation Software", published by SciTech Publishing an imprint of the IET, 2014.

[12]   *H. C. Jiang and Y.E. Wang*, "Capacity Performance of an Inductively Coupled Near Field Communication System", in Proceedings of the IEEE International Symposium of Antenna and Propagation Society, Jul. 5–11, 2008, pp. 1-4.

[13]   *M. Iordache, Lucia Dumitriu, D. Niculae, Georgiana Zainea*, "Power Transfer by Magnetic Induction Studied by Coupled Mode Theory", Book chapter in the book Wireless Power Transfer, Editor J. I. Agbinya, ISBN: 978-87-92329-23-3, River Publishers Series in Communications, Denmark, 2012, First Edition, ISBN: 8792329233, EAN: 9788792329233, pp. 1 – 40.

[14]   *M. Iordache, Lucia Dumitriu, D. Niculae, Georgiana Zainea*, "Power Transfer by Magnetic Induction Studied by Coupled Mode Theory", Book chapter in the book Wireless Power Transfer, Editor J. I. Agbinya, ISBN: 978-87-92329-23-3, River Publishers Series in Communications, Denmark, 2015, Second Edition, ISBN: 9788793237629, EAN: 9788792329233, pp. 1 – 69.

[15] *M. Iordache*, "Symbolic, Numeric – Symbolic and Numeric Simulation of Analog Circuits – User Guides", MATRIX ROM, Bucharest, 2015, ISBN 978–606–25–0126–6, 621.3.049.77.

[16] *M. Iordache, Lucia Dumitriu*, "Computer-Aided Simulation of Analoque Circuits – Algorithms and Computational Techniques", Editura POLITEHNICA Press, Vol. I and Vol. II, Bucharest 2014, ISBN 978–606-515-567-1, ISBN 978-606-515-585-5.

[17] ***http://www.keysight.com/en/pc-1297113/advanced-design-system-ads?cc=US&lc=eng.

[18] ***Agilent Technologies, AGILENT TECHNOLOGIES, Large-Signal S-Parameter Simulation, Sept. 2004.

[19] ***ANSOFT Q3D EXTRACTOR, User Guide, link: www.ANSOFT.com.

[20] ***https://www.feko.info/support.

[21] *W. Chen, R. A. Chinga, S. Yoshida, J. Lin, C. Chen and W. Lo*, "A 25.6 W 13.56 MHz wireless power transfer system with a 94% efficiency GaN class-E power amplifier", Microwave Symposium Digest (MTT), 2012 IEEE MTT-S International, Aug. 2012, pp. 1–3.

[22] *W. C. Brown*, "The history of wireless power transmission" Solar Energy, vol.56, no.1, pp. 3-21, Jan. 1996.

[23] *A. Kurs, A. Karalis, R. Moffatt, J. D. Joannopoulos, P. Fisher and M. Soijacic*, "Wireless Power Transfer via Strongly Coupled Magnetic Resonances", Massachusetts Institute of Technology, 2007 Science, Vol. 317. no. 5834, July 2007, pp. 83— 86.

[24] *R. F. Harrington*, "Field Computation by Moment Methods", Wiley-IEEE Press, 1993, ISBN: 978-0-7803-1014-8.

[25] *S. R. Pennock, P. R. Shephered*, "Microwave Engineering with Wireless Applications", McGraw-Hill Profesional © 1998, ISBN: 0070497222.

[26] ***Hewlett Packard, 1996.

[27] ***www.witricity.com.

[28] *A. K. Sah and D. P. Pant*, "Analysis and Optimization of Wireless Power Transfer Link", in Proceedings of International Conference on Technology and Innovation Management and IOE Graduate Conference, Oct. 10-11, 2014, pp. 82-93.

[29] ***http://www.nathaniyer.com/ (quick Smith); https://www.qsl.net/va3iul/ (Iulica Rosu-winsmith).

[30] *** http://www.tonnesoftware.com/supersmith.html (Tone superSmith).

[31] *L. Mandache, M. Iordache, Lucia Dumitriu, Ioana Gabriela Sirbu, D. Niculae, J. M. Paillot, D. Cordeau*, "Analysis of Coupled Ocillators through a Two-Port Passive Network", Publisher: IEEE, IEEE Xplore, Print ISBN: 978-1-4673-1809-9, Digital Object Identifier (DOI):10.1109/ICATE.2014.6972590, Page(s): 21 - 28.

[32] *V. Năvrăpescu, M. Popescu, A. I. Chirilă, I. D. Deaconu and C. Ghiţă*, "Computation Methods for Space Harmonic Effects on Single-Phase Induction Motor Performance", Rev. Roum. Sci. Techn. - Électrotechn. et Énerg., 55, No 3, Juillet-Septembre, ISSN 0035-4066, pg. 278-288, Bucureşti, 2010.

[33] *C. Ghiţă, I., D. Deaconu, A. I. Chirilă, V. Năvrăpescu and I. D. Ilina*, "2D Analysis of Electrical Transformer's Magnetic Field Due to the Magnetizing Magneto Motive Force", Rev. Roum. Sci. Techn. - Électrotechn. et Énerg., 54, No 3, Juillet-Septembre, ISSN 0035-4066, pg. 233-242, Bucureşti, 2009.

[34] *R. Carson*, "High-Frequency Amplifiers", Wiley, New York, NY, 1984.

[35] *Wai-Kai Chen*, "Active Network Analysis", World Scientific Publishing Co., 1991.

[36] *M. L. Edwards and J. H. Sinsky*, "A New Criterion for Linear 2-Port Stability Using a Single Geometrically Derived Parameter", IEEE Transactions Techniques, December 1994.

[37] *G. Lombardi, B. Neri*, "Criteria for the Evaluation of Unconditional Stability of Microwave Linear Two-Ports: A Critical Review and New Proof", IEEE Transactions on Microwave Theory and Techniques, June 1999.

[38] *D. Woods*, "Reappraisal of the Unconditional Stability Criteria for Active 2-Port Networks in Terms of S parameters", IEEE Transactions on Circuits and Systems, February 1976.

[39] *T. Ohira*, "What in the world is Q", IEEE Microwave, vol. 17, no. 6, pp. 42–49, June

2016.

[40] *T. Ohira*, "Enigmas", IEEE Microwave, vol. 17/18, 2016/2017.

[41] *T. Ohira*, "How to estimate the coupling Q factor from two-port S-parameters", in Proc. IEEE Int. Conf. Computational Electromagnetics, Kumamoto, Mar. 2017.

[42] *T. Ohira*, "The kQ Product as Viewed by an Analog Circuit Engineer", IEEE Circuits and Magazine, Vol. 17, Issue: 1, Firstquater 2017, Print ISSN: 1531-636X, DOI: 10.1109/MCAS.2016.2642698, Publisher: IEEE, pp. 27-32.

[43] *P. Wambsganß, D. Huwig*, "A New Figure of Merit and General Properties of Wireless Power Transmission Systems",
Link: www.etatronix.de/wp-content/.../etatronix_paper_2014.pdf.

[44] *M. Rehman, Z. Baharudin, P. Nallagownden, B. Islam, M. Z. Ur Rehman*, "Modeling and Analysis of Series-Series and Series-Parallel Combined Topology for Wireless Power Transfer using Multiple Coupling Coefficients", IJCSNS International Journal of Computer Science and Network Security, VOL.17 No.11, November 2017, pp. 114-123.

[45] *Mihai Iordache, Lucia Dumitriu, Dragos Niculae, Marilena Stanculescu, Victor Bucata, Georgiana Razmerita* – Capitolul "Circuit Analysis with nullors", în cartea M. Fakhfakh, M. Pierzchala – editors, "Pathological Elements in Analog Circuit Design", Springer U.S., 2018, pag. 91-147, ISBN 978-3-319-75157-3; 978-3-319-75156-6.

[46] *Marilena Stanculescu, Lavinia Bobaru, Dragoş Niculae, Sorin Deleanu, Victor Bucată, Mihai Iordache* - Coordonator, "*Wireless Electromagnetic Energy Transfer Systems*", MATRIX ROM, Bucharest, 2021, ISBN 978 – 606 – 25 – 0623 - 0, 621.3.

[47] *Mihai Iordache, Marilena Stănculescu, Dragoş Niculae, Maria-Lavinia Iordache (Bobaru), Răzvan Asanache*, "Switched Networks Analysis with Inconsistent Initial Conditions", Modern Power Systems, Cluj, 06-09.06.2017, PID4766833.

[48] *Ciprian Curteanu, Maria-Lavinia Iordache (Bobaru), Răzvan Asanache, Mihai Iordache, Marilena Stanculescu*, "*S*-Parameters utilization in electrical quadrupoles analysis", Electronics, Computers and Artificial Intelligence, Targoviste, 29.06-01.07.2017, paper 61.

[49] *Răzvan Asanache, Mihai Iordache, Dragoş Niculae, Marilena Stănculescu, Maria Lavinia Bobaru, Victor Bucată*, "The computation of the kQ-product and properties of wireless power transfer systems", International Conference on Applied and Theoretical Electricity, Craiova, 04-06.10.2018, ID134.

[50] *Răzvan Asanache, Mihai Iordache, Dragoş Niculae, Marilena Stănculescu, Lavinia Bobaru, Victor Bucată*, "On Circuit Analysis and Simulation of Networks with Nullors", Modern Power Systems, Cluj, 21-23.05.2019, ID169.

[51] *Răzvan Asanache, Cristina Mihaela Turcu, Mihai Iordache*, "Automatic Generation of Linear Quadrupole Parameters", U.P.B. Scientific Bulletin Series C: Electrical Engineering and Computer Science, iunie 2020, ID: 9381.

[52] *Răzvan Asanache, Mihai Iordache, Mihaela Cristina Turcu, Alexandru Grib, Lucian Vasile Ene, Diana Ramona Sănătescu*, "Wireless Charging Systems for Electrical Vehicle Batteries", Electronics, Computers and Artificial Intelligence, 2020, e-Session, ID: 55.

[53] *Mihaela Cristina Turcu, Mihai Iordache, Răzvan Asanache, Alexandru Grib, Teodor Cătălin Bibirică*, "Smart Integrative System for the Battery Balance Monitoring", Electronics, Computers and Artificial Intelligence, 2020, e-Session, ID: 56.

[54] *Alexandru Grib, Mihai Iordache, Răzvan Asanache, Mihaela Cristina Turcu, Teodor Cătălin Bibirică*, "Smart Battery Monitoring System Software Design", Electronics, Computers and Artificial Intelligence, 2020, e-Session, ID: 97.